COMPUTER SIMULATION OF MASS TRANSPORT IN GROUNDWATER:
AFFECT OF MACROSCOPIC HETEROGENEITIES IN HYDRAULIC CONDUCTIVITY

APPROVED:

_____

_____

_____

COMPUTER SIMULATION OF MASS TRANSPORT IN GROUNDWATER: AFFECT OF MACROSCOPIC HETEROGENEITIES IN HYDRAULIC CONDUCTIVITY

BY

PETER B. MCMAHON, B.S.

THESIS

Presented to the Faculty of the Graduate School of

The University of Texas at Austin

in Partial Fulfillment

of the Requirements

for the Degree of

MASTER OF ARTS

THE UNIVERSITY OF TEXAS AT AUSTIN

May, 1984

ACKNOWLEDGMENTS

I would like to thank my advisor Dr. John M. Sharp, Jr. and committee members Dr. Randy Charbeneau and Dr. Charlie Kreitler for their technical and grammatical review of this project. To Dr. Sharp for his moral and monetary support, and Dr. Charbeneau for the use of the Trescott model.

To all of the wonderful people associated with the University of Texas Geology Department, I say thank you. There was never a lack of friendship, stimulating conversation, or arm-waving on the fourth floor. Special recognition belongs to Paul Blanchard, Pamela Tiezzi, and Jay Vogt.

Finally, I would like to express special gratitude to my parents, Rachel and Jerry, for their constant love.

Submitted to Committee: 23 March 1984

ABSTRACT

In this study a computer model was used to simulate dissolved chloride movement through alluvial sediments which border the Canadian River in Hutchinson County, Texas. Hydraulic conductivity values of the sediments were required in order to calculate groundwater velocities in the system. The most realistic representation of conductivity variations in porous media is expressed by frequency distributions rather than by averaged values of conductivity. Numerous sedimentological environments exhibit log-normal conductivity distributions; therefore, one was used in this investigation.

A number of conclusions can be based on the results of this study. First, certain conductivity distributions account for the observed spread of chloride in the aquifer. The best match of observed chloride dispersion was obtained with autocorrelated log-normal conductivity distributions. Secondly, the degree of spatial dependence between adjacent conductivity values affected numerous results. These include the amount of chloride dispersion and the extent of uncertainty in calculated hydraulic head and chloride distributions.

For comparative purposes the chloride distribution was also modeled using an average conductivity value. Under this condition the chloride plume moved at an average rate of 10 meters/year. Another result was that longitudinal and transverse dispersivities of 46 meters and 9 meters, respectively, were required to obtain a match between observed and modeled chloride distributions.

TABLE OF CONTENTS

LIST OF TABLES

LIST OF FIGURES

I. INTRODUCTION

The potential exists for large scale contamination of groundwater resources in the United States. In fact, nearly 1.7 trillion gallons of waste are placed in the ground in the U.S. each year (U.S. EPA, 1977). It would be desirable, therefore, to understand how mass is transported in groundwater. One approach is to use computer models to simulate mass transport in groundwater. Unfortunately, currently applied modeling techniques do not describe the actual processes of mass transport in porous media.

Most computer models are deterministic. A deterministic model is one in which none of the input parameters are variable (Freeze, 1975). For example, the hydraulic conductivity range of a porous medium would be represented by an averaged hydraulic conductivity value. The purpose of this study was to simulate the movement of dissolved chloride at a site of groundwater contamination in North Texas by using a stochastic computer model of mass transport in porous media.

A stochastic model is one in which the input parameters are described statistically in terms of the mean and standard deviation of the parameter's distribution in the system being modeled. In this study hydraulic conductivity was described statistically and used as input in the stochastic computer model. Furthermore, the hydraulic conductivity was assumed to follow a log-normal distribution (Smith and Freeze, 1979).

II. OBJECTIVES

The objectives of this study were both theoretical and field oriented.

The theoretical objectives were 1) to quantify the effect of different log-normal hydraulic conductivity distributions on mean hydraulic head and dissolved chloride distributions; 2) to examine the uncertainty in head and chloride distributions produced by different log-normal conductivity distributions; 3) to study the effect of changing the conductivity distributions on groundwater velocities.

My field objectives were 1) to model the observed chloride distribution deterministically. In doing this the longitudinal and transverse dispersivities required to obtain a match between observed and calculated chloride distributions would be determined. I also wanted to model the system stochastically. If the stochastic model could produce the same amount of mixing as the deterministic model, but with smaller dispersivities, the mixing must be created by the large-scale hydraulic conductivity variations created by the stochastic model. Large-scale conductivity variations in porous media are responsible for field-scale mixing of mass in groundwater (Schwartz, 1977).

III. THEORY AND MECHANISMS OF MASS TRANSPORT

The success of a computer model in predicting contaminant distributions in groundwater systems is dependent upon the model's ability to accurately describe the dispersive character of the natural system. Mass transport in saturated porous media occurs through the processes of advection and hydrodynamic dispersion. Advection moves particles

directly with the average velocity of the flowing groundwater. Hydrodynamic dispersion moves particles by mechanical mixing and molecular diffusion. Molecular diffusion is the mechanism whereby molecules move in response to a concentration gradient. Mechanical mixing is created by microscopic variations in fluid velocity within the pore spaces of the medium.

Computer models of mass transport in porous media are based upon a partial differential equation describing mass transport. The deterministic model requires using dispersivities in the differential equation. The dispersivity is a property of the porous medium and is a measure of the medium's ability to transport and spread dissolved chemical species in groundwater. Dispersivities can also be thought of as indicators of the uncertainty in groundwater velocity in the system (Domenico and Palciauskas, 1979). Gillham and Cherry (1982) stated that the observed degree of spreading of a contaminant in groundwater is generally much greater than would be predicted by using laboratory-scale dispersivities. Dispersivities determined in laboratory experiments are on the order of centimeters while those used to describe field-scale mixing are on the order of meters (Wang and Anderson, 1982). Field-scale dispersivities are determined from trial-and-error approximations of field data.

The dispersion portion of the classical governing equation of mass transport, in which these dispersivities are used, is based on the assumption that macroscopic dispersion is analogous to Fick's law of diffusion. The problem lies in the fact that modeling large-scale dispersion as a diffusion phenomenon is commonly an incorrect approach

to a different and considerably more complex process (Smith and Schwartz, 1980). Research into the nature of mass transport in macroscopically heterogeneous porous media is just beginning to examine this problem in detail.

The velocity field which provides the advective motion of mass transport is described mathematically by Darcy's law and the groundwater flow equation (Mercer and Faust, 1981).

$$\tilde{v} = -\tilde{\tilde{K}} / \phi \cdot \nabla h \tag{1}$$

$$\nabla \cdot \tilde{\tilde{K}} \cdot \nabla h + R = S_s \, \partial h / \partial t \tag{2}$$

Where, $\tilde{v}$ is the average linear groundwater velocity, $\tilde{\tilde{K}}$ is the hydraulic conductivity tensor, h is the hydraulic head, ϕ is porosity, R is a source/sink term (e.g. water wells, rivers, evaporation ponds, evapotranspiration), and S_s is the specific storage of the medium (see Appendix A for a complete listing of all symbols and their units used in this paper). The derivation of these equations follows a continuum approach in that the actual ensemble of grains is replaced by a representative volume (Freeze and Cherry, 1979, p. 69).

In other words, the parameters and boundary conditions required to solve these equations cannot be defined at every point in the system so they must be averaged over a representative volume of the medium. For example, a constant porosity cannot be defined for a volume of porous medium that is smaller than its representative volume (Freeze and Cherry, 1979, p. 69). This introduces error in the calculations.

Hubbert (1940, p. 59) addressed the conditions under which these equations provide reasonable results. In general, a good representation of the bulk fluid motion can be obtained for many systems of saturated porous media. This is not the case for many types of fractured media.

Molecular diffusion is described by Fick's law of diffusion.

$$F = -D\nabla C \tag{3}$$

Where, F is the mass flux, D is the coefficient of molecular diffusion, and C is the concentration of dissolved chemical species.

Ideally, fluid velocities within the individual pores should be determined in order for mechanical mixing to be accurately described. As stated above, however, only average velocities can be determined (Schwartz, 1977). Bear (1979, p. 232) showed that the spatial averaging of the local, microscopic mass flux ($\overline{Cv}$) due to velocity variations within pore spaces is:

$$\overline{Cv} = \bar{C}\,\bar{v} + \overline{\mathring{C}\,\mathring{v}} \tag{4}$$

The first term on the right represents the average advective flux, where the average velocity is calculated with equation (1). The second term represents the spatially averaged fluctuation from $\bar{\bar{C}}\bar{v}$, or, the dispersive flux. Mechanical mixing is represented by the second term in equation (4). It is assumed that the dispersive flux is analogous to Fick's law of diffusion (Bear, 1979, p. 232). This is represented by equation (5).

$$\overline{\mathring{C}\,\mathring{v}} = -\bar{\bar{D}} \cdot \nabla C \tag{5}$$

The coefficient $\bar{\bar{D}}$, a second order tensor, is the coefficient of mechanical dispersion. Scheidegger (1961) proposed the following relationship for the coefficient of mechanical dispersion.

$$D_{ij} = \alpha_t |v| \delta_{ij} + (d_l - d_t) \frac{v_i v_j}{|v|} \tag{6}$$

Where, d_t is the transverse dispersivity, d_l is the longitudinal dispersivity, v_i is the component of groundwater velocity in the i-th direction, v_j is the component of groundwater velocity in the j-th direction, δ_{ij} is the Kronecker delta ($\delta_{ij}=1$, if $i=j$; $\delta_{ij}=0$, if $i\neq j$), and v is the magnitude of the groundwater velocity vector resulting from the addition of v_i and v_j. Equation (6) assumes homogeneous, isotropic dispersion. Since $\theta=\tan^{-1}(v_y/v_x)$, equation (6) may be written as:

$$D_{xx} = d_l v \cos^2\theta + d_t v \sin^2\theta \tag{7}$$

$$D_{xy} = (d_l - d_t) v \sin 2\theta \tag{8}$$

$$D_{yy} = d_l v \sin^2\theta + d_t v \cos^2\theta \tag{9}$$

If flow is oriented in the x-direction (i.e. $\theta=0$); $D_{xx}=d_l v$, $D_{yy}=d_t v$, and $D_{xy}=0$. The velocities in equation (6) are calculated with equation (1).

In order for mechanical mixing to be approximated as a diffusional process it must follow the fundamental statistical model of diffusion.

Bear (1972, p. 589) showed that as

> total particle travel time becomes much larger than the time interval during which its local velocities are still correlated, the total displacement may be considered as a sum of a large number of elementary displacements statistically independent of one another. Then the probability distribution of the particles' total displacement tends to the normal (Gaussian) distribution.

This means that a package of tracer particles will converge to a normal distribution and spread with a variance that is proportional to time, or the distance moved, lenght=vt (Smith and Schwartz, 1980). Prickett and others (1981) describe this mathematically with equations (10) and (11).

$$C(x,t) = \frac{1}{(4\pi d_\ell v t)^{1/2}} \exp\left[-\frac{(x-vt)^2}{4 d_\ell v t}\right] \qquad (10)$$

$$n(x) = \frac{1}{(2\pi\sigma)^{1/2}} \exp\left[-\frac{(x-u)^2}{2\sigma^2}\right] \qquad (11)$$

Where, σ is the standard deviation of the normal distribution, u is the mean of the normal distribution, n(x) is the density function of a normal distribution, and all other terms were defined previously. Equation (10) is the solution to the one-dimensional mass transport equation, and equation (11) is the density function for a variate, x, that is normally distributed. Equations (10) and (11) are equivalent. Further equivalencies are given by equations (12) and (13).

$$\sigma^2 = 2 d_\ell v t \qquad (12)$$

$$u = vt \tag{13}$$

Equation (12) states that the variance of the normal distribution is linearly proportional to the mean displacement of mass in a given time step, vt. One-half the slope of this linear relationship is the longitudinal dispersivity, d_l. Equation (13) shows that the mean advective displacement is equal to the mean of the normal distribution.

Mass transport in laboratory columns and most other homogeneous porous media is described well by the statistical model of mechanical mixing because the travel time during which the local velocities are still correlated, as described by Bear (1972, p. 589), is short. This means that the assumptions upon which the statistical model are based, are valid after short travel distances. If the heterogeneities of the medium increase in size, the travel time during which local velocities are still correlated increases. Therefore, the assumptions are valid only after large travel times. For example, suppose sampling for a dissolved chemical species in groundwater is to be done over a segment of an aquifer composed of fluvial sediments. The aquifer is likely to consist of relatively high conductivity channel sands (probably interconnected) surrounded by lower conductivity interchannel muds (Galloway and Kaiser, 1980). Furthermore, let us say that the dissolved chemical species is injected continuously within a channel sand body. A normal distribution of the chemical is likely to be observed early on as the

injected chemical is transported through the relatively homogeneous sand (Fig. 1c). However, as the chemical is transported through larger heterogeneities, the Gaussian chemical distribution will break down (Fig. 1b). A normal distribution of the dissolved chemical species will not be observed again until a large enough time has passed so that the chemical has been dispersed equally throughout the aquifer (Fig. 1a).

Because the components of mass transport due to molecular diffusion and mechanical mixing are now in the same form, they are combined into a single expression the coefficient of which is called the coefficient of hydrodynamic dispersion.

$$\tilde{\tilde{D}}_h = D\delta_{ij} + D_{ij} \tag{14}$$

The final form of the governing equation of mass transport in a saturated porous medium is (Mercer and Faust, 1981):

$$\nabla \cdot \tilde{\tilde{D}}_h \cdot \nabla C - \nabla \cdot \tilde{v} C + W = \partial C / \partial t \tag{15}$$

The first term on the left represents dispersion caused by molecular diffusion and mechanical mixing. For velocities found in most groundwater systems molecular diffusion is negligible in comparison to mechanical mixing. The second term represents advective transport caused by groundwater flow. If the velocities in this term were exact (i.e. not

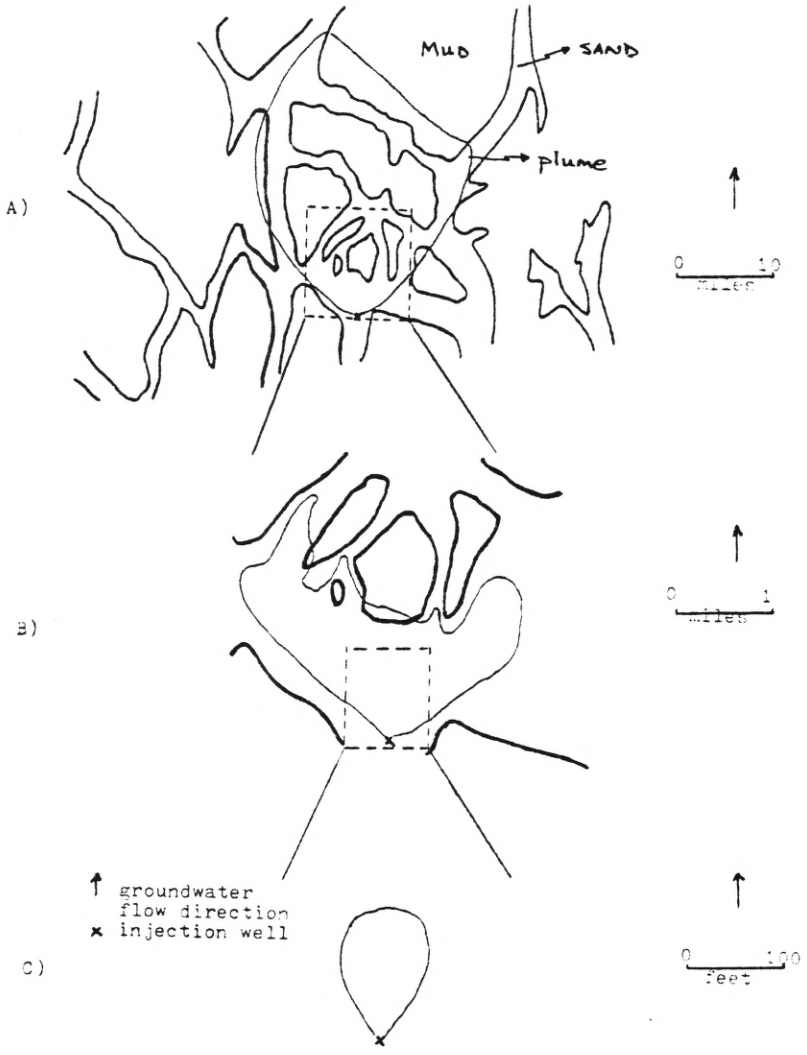

Figure 1. Cartoon illustrating scale-dependent dispersion in a heterogeneous porous medium.

spatially averaged), the mechanical mixing portion of (15) would not be needed and the transport of mass could be described by the processes of advection and molecular diffusion (Pickens and Grisak, 1981). Sources and sinks are included in the third term of equation (15). Possible sources and sinks are chemical and biological reactions, adsorption, recovery wells, and leakage from surface water bodies. The righthand side of equation (15) represents the time rate of change of mass stored in the system.

The inadequacies encountered in using dispersivities to account for large-scale mixing can be summarized as follows. The assumption that macroscopic dispersion is analogous to Fick's law of diffusion is frequently invalid for transport in heterogeneous porous media. Schwartz and others (1983) found that "Gaussian distributions of mass predicted by the diffusional model of dispersion are only observed under a very narrow range of conditions." Secondly, dispersivities do not remain constant as the scale of heterogeneities changes. This means that dispersivities used to obtain a match between observed and calculated mass distributions at one point in time may not give a match at a later time. Molz and others (1983) attempted to use scale dependent dispersivities in equation (15) in order to describe mass transport in a stratified porous aquifer. They determined that the longitudinal dispersivity would not approach an asymptotic value until a travel distance of 109 kilometers had been reached. Schwartz (1977) found that constant dispersivities could not be obtained in a medium containing high or low conductivity lenses unless those lenses were arranged homogeneously within the system. Finally, merely adjusting dispersivities to obtain

a match gives no insight into the processes of mixing in heterogeneous porous media.

Field-scale mixing is caused by large-scale porous media heterogeneities which are responsible for changes in the direction and velocity of groundwater flow. If you could incorporate the distribution of heterogeneities in your model, instead of using average conductivities as obtained from pump tests, many of the inadequacies of the deterministic model could be reduced, if not eliminated. Stochastic modeling techniques can do this.

A stochastic model is one in which the input parameters are described statistically in terms of the mean and standard deviation of the parameter's distribution in the system being modeled. In this study hydraulic conductivity was described statistically in terms of the mean and standard deviation of the conductivity distribution in the system and used as input in the stochastic computer model.

In describing the hydraulic conductivity distribution statistically it must be realized that there are an infinite number of conductivity distributions that can be created having the same mean and standard deviation. Therefore, without more data with which to eliminate inappropriate K distributions from the system being modeled, any one conductivity distribution is as realistic as the next. For this reason, equations (1), (2), and (15), as used in the stochastic model, were solved 20 times, each time using a different hydraulic conductivity distribution from a family of distributions having the same mean and standard deviation. The resulting averages of the hydraulic head and

dissolved chloride distributions were examined.

The average of 20 samples from a log-normal distribution (σ =0.55) of hydraulic conductivities yielded a conductivity value at each node within 0.25 log units, based on a 95% confidence level, of the geometric mean of the log-normal distribution (Daniel, 1977, p. 142). For the geometric mean of 5.2 meters/day used in this study this translated to a conductivity value between 2.9 and 8.9 meters/day. In other words, the K value assigned to any node of the finite difference grid could vary greatly for any one conductivity distribution. However, the average K value (averaged over 20 runs) approached the geometric mean of the conductivity distribution.

IV. GEOLOGY

My study site is located along the Canadian River in Hutchinson County, Texas (Figs. 2 and 3). It is situated adjacent to state highway 2277 about halfway between Stinnett and Borger, Texas (Fig. 4). The river forms the Canadian River Basin of the Northern Panhandle. The basin is part to the North Plains and Southern High Plains topographic features within which elevations range between 4735 feet and 2167 feet above mean sea level (Manford et al., 1974).

The average effective rainfall in the basin for the period 1940-1957 was 19.2 inches while the average gross evaporation rate for the same period was 73.9 inches (Manford et al., 1974).

Structurally, the study area lies within the western edge of the Anadarko Basin (Fig. 5). To the south and west are the Amarillo Uplift and Dalhart Basin, respectively. The tectonic activity that created the

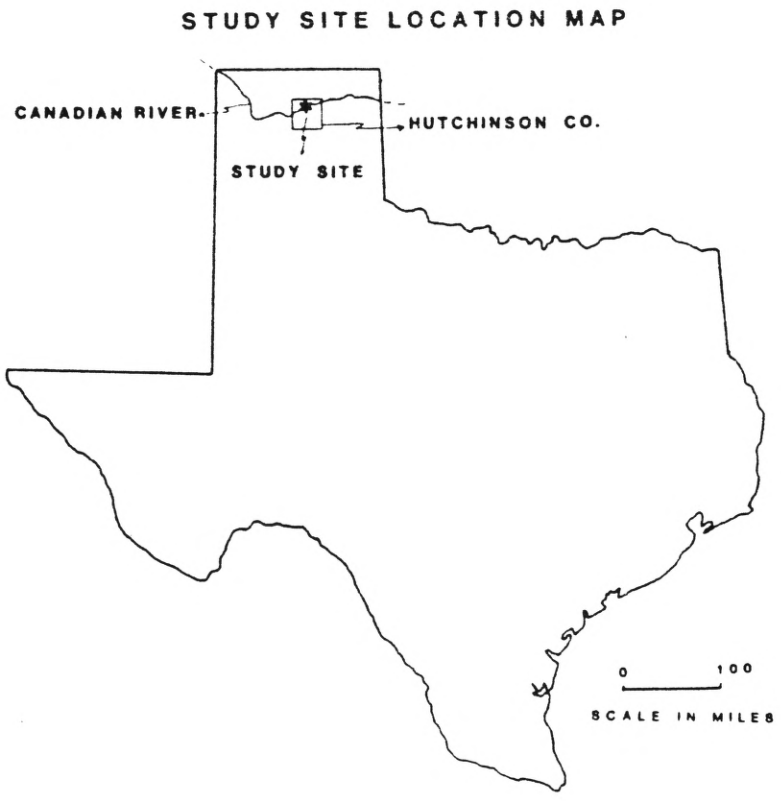

Figure 2. Map showing location of study site in Texas.

Figure 3. Photograph of the Canadian River and its floodplain. Picture taken from highway 2277 bridge looking west.

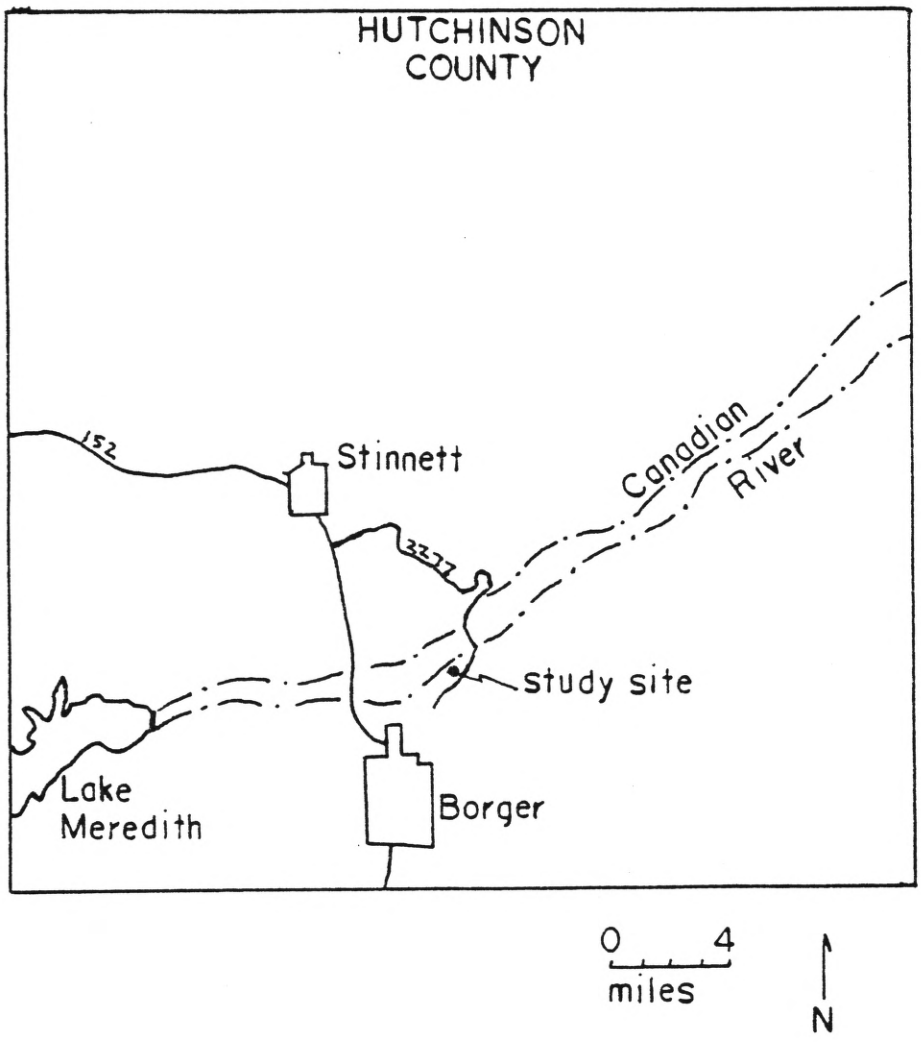

Figure 4. Map showing location of study site in Hutchinson County, Texas.

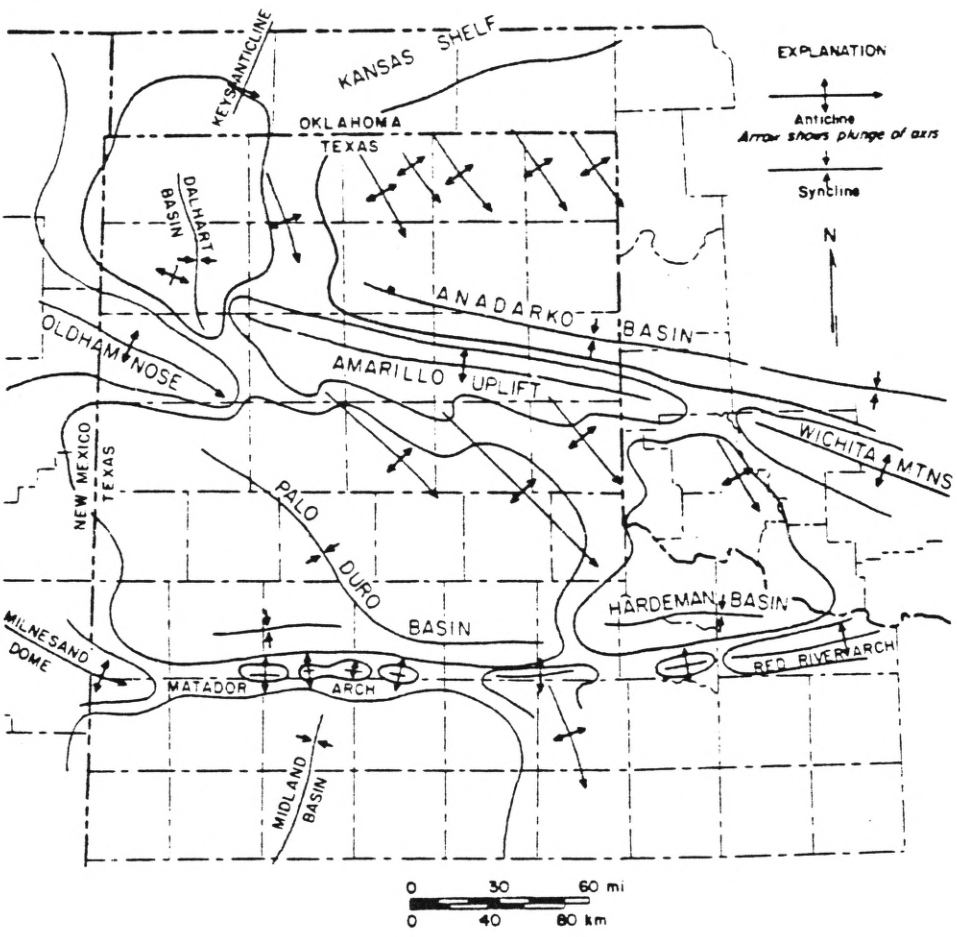

Figure 5. Map showing structural features of Texas Panhandle (after Gustavson, 1980a).

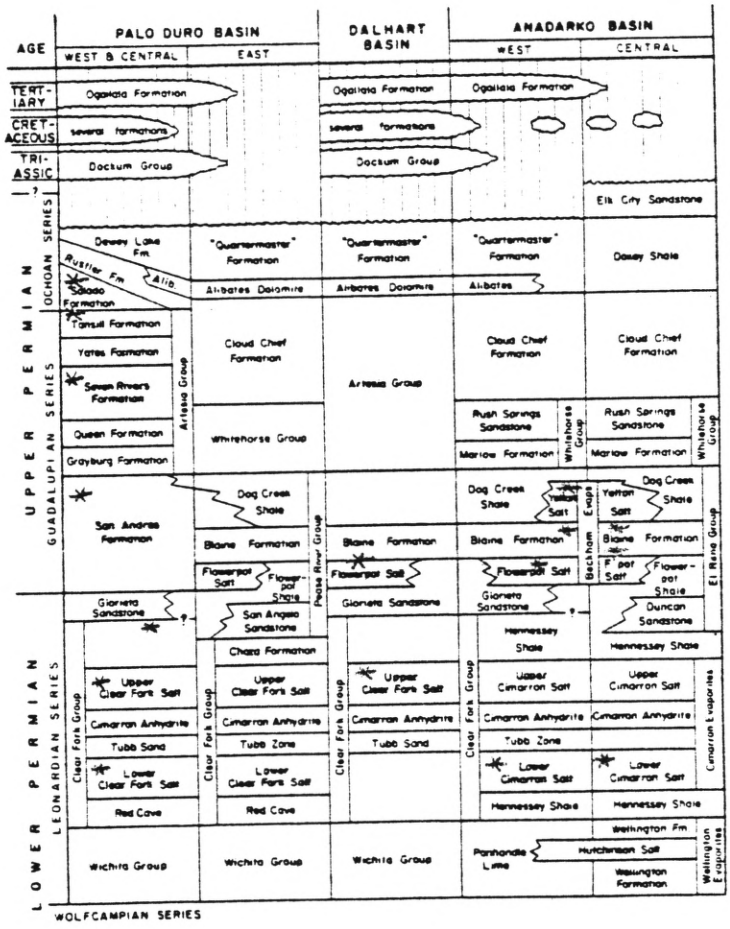

Figure 6. Stratigraphic columns of the major basins of the Texas Panhandle (after Gustavson, 1980a).

arches, domes, and basins of the Texas Panhandle occurred primarily during Pennsylvanian time (Gustavson et al., 1980a). Minor movements have occurred, however, since Permian time. These movements are attributed to differential compaction of basin sediments and/or post-tectonic adjustment of the earth's crust (Gustavson et al., 1980a).

Stratigraphic columns are shown in Figure 6 for the three major sedimentary basins of the Texas Panhandle. Most of the fresh groundwater in the Anadarko Basin occurs within the sands and gravels of the Ogallala Formation of Tertiary age. Substantial amounts of water can also be found in Cretaceous, Jurassic, and Triassic rocks underlying the Ogallala. Subsurface portions of the Permian formations contain groundwater that generally is poor and exceeds the water-quality standards set by the U.S. Public Health Service for drinking water (500 mg/l TDS in most places; Richter, 1983). Finally, minor supplies of groundwater have been taken from alluvial sediments of Quaternary age which border the Canadian River.

The study site is located in a major salt dissolution zone within the Texas Panhandle. The evaporite deposits are located in the Permian strata of the Anadarko, Dalhart, and Palo Duro basins (Gustavson et al., 1980a). Overall, the Permian beds are composed of salt, anhydrite, dolomite, limestone, and red beds. The red beds consist of mudstones and fine-grained sandstones that intertongue with evaporites and dolomite (Gustavson et al., 1980a). The seven salt-bearing units within the basins are marked by asterisks in Figure 6. With the probable exception of the lower Cimarron Salt, all of the younger salt-bearing units are

undergoing salt dissolution on a regional scale (Gustavson et al., 1980a). Gustavson and others (1980a) list several lines of evidence to support salt dissolution in the Anadarko basin. Included are major collapse chimneys at the Lake Meredith dam and along highway 152 between Stinnett and Borger (Fig. 4). The collapse chimneys occur in Permian mudstones and are filled in with Tertiary or younger sediments. Collapse occurs because of dissolution of the underlying salt by groundwater. The extremely high salt loads carried by the rivers of the Texas Panhandle also suggest dissolution of subsurface salt and discharge of these saline groundwaters at the land surface. The mean annual salt load carried by the Canadian River at Amarillo is 6.9542×10^5 cubic feet of halite (Gustavson et al., 1980b).

Dissolution of Permian evaporites by groundwater has major implications for groundwater chemistry in the Texas Panhandle. Richter (1983) studied the geochemical characteristics of salt-spring and shallow subsurface brines in that portion of the Panhandle to the south of my study area. He was able to delineate two distinct brine bodies in the subsurface in his study area. Halite dissolution by local, meteoric fresh groundwater accounts for a brine body which underlies his study area at shallow depths. This is a Na-Cl brine with sulfate as the third major component. The chemistry of the brine is generally believed to be controlled by halite and to some degree by gypsum/anhydrite (Richter, 1983). The brine discharges as salt springs and salt seeps in topographically low places within his study area. Discharge of deep-basin brine aquifers into overlying units accounts for a shallow subsurface brine in the

southern portion of his study area. The deep-aquifer brine can be subdivided into two brine-types; a Na-Cl type and a Na-Mg-Cl type. It is only in the southern part of his study area that hydraulic heads of the deep-basin aquifer are large enough to allow the deep brines to approach land surface (Richter, 1983). Richter (1983) also presented evidence for a third brine-type which represents mixing of the two previously described brines. Spatially, the salinity of salt-spring brines varies considerably between major salt-emission areas and between springs in individual emission areas (Richter, 1983). Chloride concentrations reported by Richter in springs within his study area range from about 5,300 mg/l to over 192,000 mg/l.

Caustic brine wastes produced by Phillips Petroleum Company as part of its oil refining process had been disposed of since 1940 in an 11-acre evaporation pond (Fig. 7, Geogulf, 1981). Leakage of the waste through the pond bottom had caused contamination of the groundwater in the underlying alluvial sediments. The primary contaminants are dissolved chloride and organics.

The alluvial sediments were deposited by the Canadian River which is a braided stream in this part of the Texas Panhandle. The river flows in a shallow valley cut into Permian shale, siltstone, and dolomite of the Doxey Shale and the Cloud Chief Formation in Hutchinson County; and gravel, sand, and silt of the Ogallala Formation in most of the remainder of the basin.

The floodplain deposits of the Canadian River are preserved in at least eight channel sequences of varying age which represent recent

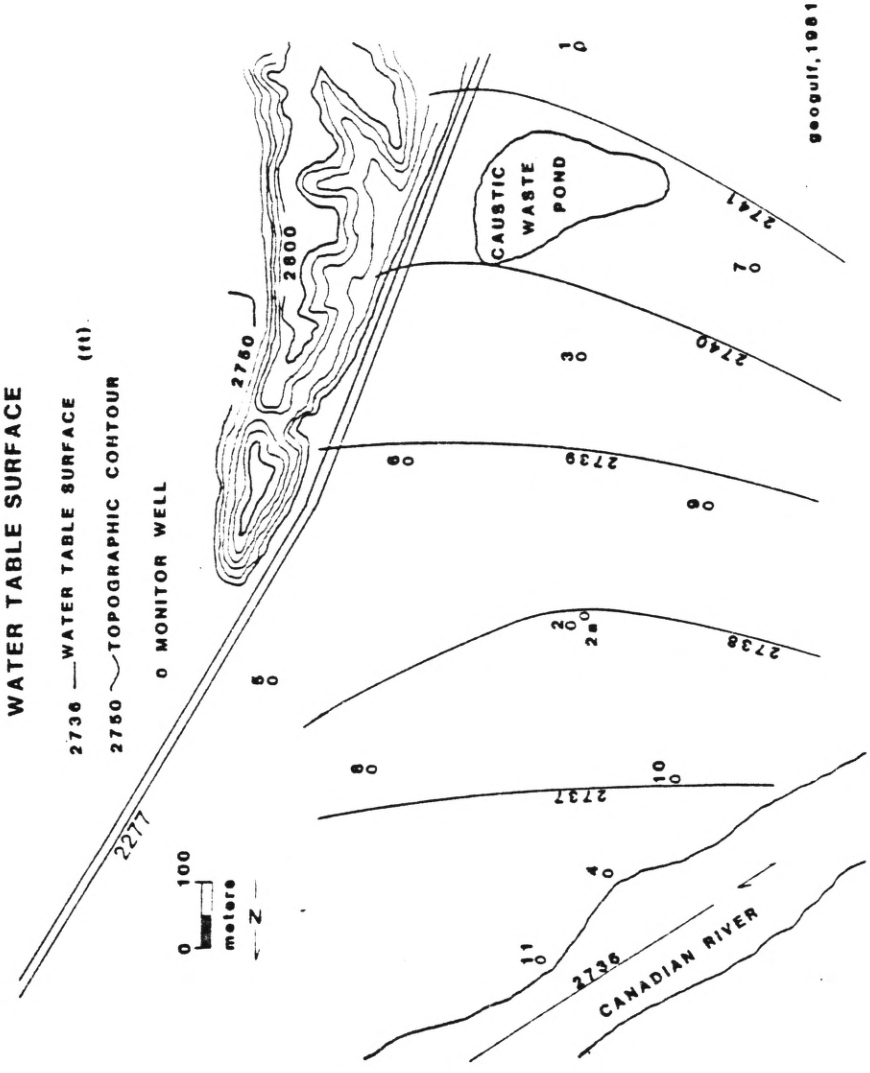

Figure 7. Water table surface and location of monitor wells at study site (after Geogulf, 1981).

major flood events (Kessler, 1971). The braided and aggradational nature of the deposits is a function of the river's incompetence to carry a heavy sediment load. The source of the sediments is undercutting of incompetent bank material such as the Permian shale, the weakly consolidated sediments of the Ogallala and older river channel deposits (Kessler, 1971). The braided stream deposits are up to 40 meters thick at the study site (Fig. 8, Geogulf, 1981). The sediments consist of unconsolidated gravel, sand, silt, and clay. They are underlain by Permian redbeds. A recovery test performed at monitor well 2 (MW-2) by Geogulf (1981) yielded an average hydraulic conductivity for the sediments of 5.2 meters/day. The water table contour map, along with monitor well locations, is shown in Figure 7. The water table contours indicate that groundwater is flowing from the region of the evaporation pond to the Canadian River.

A visit to the study area on 30 November 1983 showed that the site has undergone major changes. The outcrop of Permian redbeds along highway 2277 has been used to fill in the evaporation pond. Therefore, the groundwater is nolonger receiving contaminated water from the pond. Furthermore, three recovery wells have been placed in an east-west line downgradient of the pond (between MW-3 and MW-6) in order to remove contaminated groundwater from the alluvium (Fig. 9).

V. ASSUMPTIONS

Two major assumptions concerning the hydraulic conductivity distribution used in the stochastic model were made in this study.

I assumed that hydraulic conductivities in the braided stream deposits are log-normally distributed. There is good evidence to support

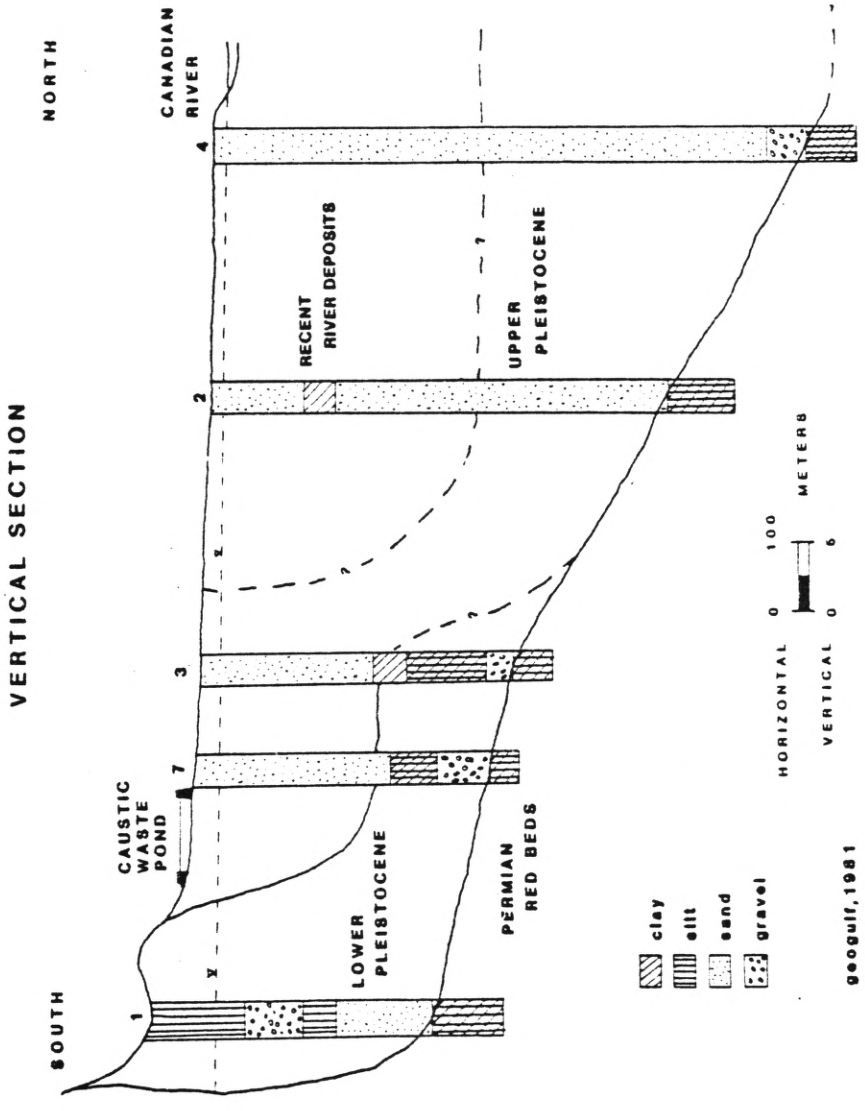

Figure 8. Cross section from the pond to the Canadian River (after Geogulf, 1981).

Figure 9. Photograph showing pond closure operations.

this assumption. Freeze (1975) summarized the evidence. Based on core data Law (1944) found conductivities in a carbonate oil reservoir to be log-normally distributed. Bulnes (1946) and Warren and others (1961), also working with cores, supported Law's findings. Transmissivity maps of the Los Angeles basin showed conductivities to be log-normally distributed (McMillan, 1966). An analysis performed by Bennion and Griffiths (1966) of 60,000 cores from 2,000 wells in a sand and gravel oil reservoir and 24,000 cores from 430 wells in a limestone reservoir showed hydraulic conductivities in those reservoirs to be log-normally distributed.

Indirect evidence supports a log-normal distribution for hydraulic conductivities. Davis (1969) noted that specific capacities of water wells (which are directly related to transmissivities) are usually log-normally distributed. Grain-size distributions are log-normal and can be related to conductivities in a functional way (e.g. the Carmen-Kozeny equation)(Freeze, 1975). In fact, the ø (phi) scale of grain-size classification was developed for the reason that grain-sizes are log-normally distributed (Folk, 1954). Pollack (1961) found grain-sizes of the braided stream deposits of the Canadian River in and near my study area to be log-normally distributed.

The second major assumption of my stochastic model was that the geometric mean of the hydraulic conductivity distribution in the alluvial sediments was determined by the recovery test performed at MW-2. This assumption was supported by theoretical studies both described in the literature and performed by myself.

Warren and Price (1961) used a three-dimensional model to simulate

a pressure build-up test in a medium having a random log-normal conductivity distribution. They found that the conductivity determined from the build-up test gave a reasonable value for the geometric mean of the conductivity distribution. Smith and Freeze (1979) quoted two studies in which the effective conductivity of a porous medium was found to be equal to the geometric mean of the hydraulic conductivity distribution. The effective hydraulic conductivity is a single value that could replace the spatially variable conductivity distribution while preserving the hydraulic behavior of the original medium (Smith and Freeze, 1979). Smith and Freeze (1979) state that hydraulic equivalency requires 1) the mean value of head at any point, as determined from a stochastic solution, must equal the head value at that point, as determined from a single deterministic solution using the effective conductivity of the medium and 2) the mean value of any flow measurement, such as flux, from a stochastic solution must equal the single value provided by the deterministic model.

I simulated a simple pump test using a 3-D model in which the conductivities followed a random log-normal distribution. This was done in order to determine if the geometric mean of a log-normal hydraulic conductivity distribution could be determined from a pump test. The mean of the log-normal distribution was 26.2 meters/day and the standard deviation was 0.55 meters/day (this standard deviation is in log units). The aquifer was infinite in areal extent and the well was fully penetrating. The three-dimensional pump test simulations were performed with the USGS flow model written by Trescott (1975). Because no changes were made in the 3-D model as listed in Trescott (1975), it was not included

in the Appendices. The model represented a cube with no-flow boundaries on all sides and the bottom. The infinite aquifer was simulated by placing the lateral no-flow boundaries sufficiently far apart so that the boundary effects were not felt by the pumping well. The initial condition was a constant water level throughout the system. Pumping was then started using a constant pumping rate of 60 cubic feet/minute. The grid spacings in the x- and y-directions were taken as 1000 feet for model 1 and 100 feet for model 2. The change in the z-direction was held at 100 feet in both models.

The well was pumped for 24 hours. A plot of the resulting time-drawdown data on semi-log graph paper yielded a straight-line relationship. Transmissivities were calculated from these data according to Jacob's method (Cooper and Jacob, 1946). Thirty-five pump tests were performed for each model. For every pump test a different conductivity distribution was taken from a family of distributions having the same mean and standard deviation.

The results of the first model are shown in Figure 10. In this case the grid spacing in the x- and y-directions was 1000 feet. The average conductivity (K_a) obtained from the 35 tests was very similar to the geometric mean (K_g) of the log-normal conductivity distribution. However, there was a good deal of deviation (σ=12.5 meters/day) between conductivities determined from individual pump tests.

The pump test results obtained with the grid spacing in the x- and y-directions set at 100 feet are shown in Figure 11. Again the average conductivity determined from the 35 tests was nearly equal to the

PUMP TEST RESULTS

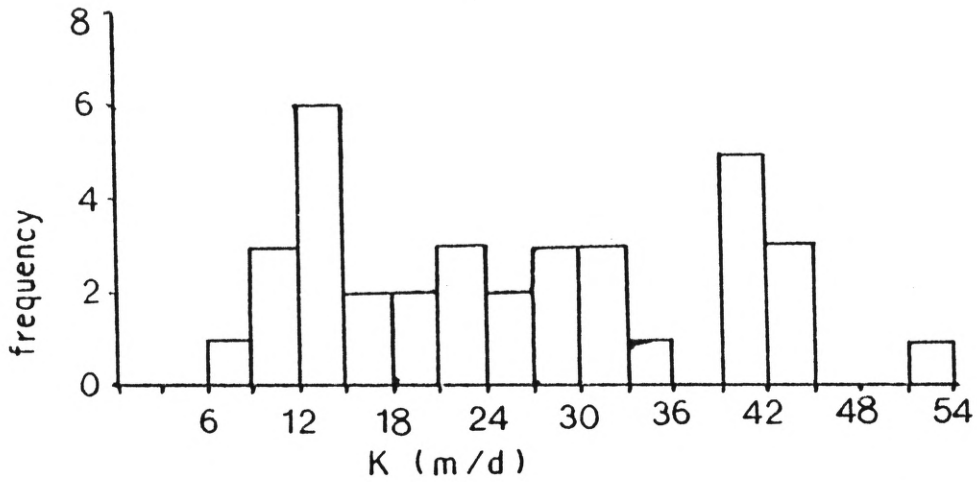

$n = 35$

$Q = 60\ ft^3/min$

$\Delta x = \Delta y = 1000\ ft$

$\Delta z = 100\ ft$

$K_g = 26.2\ m/d$

$K_a = 26.8\ m/d$

$\sigma = 12.5\ m/d$

Figure 10. Three-dimensional pump test modeling results, delx and dely equal 1000 feet.

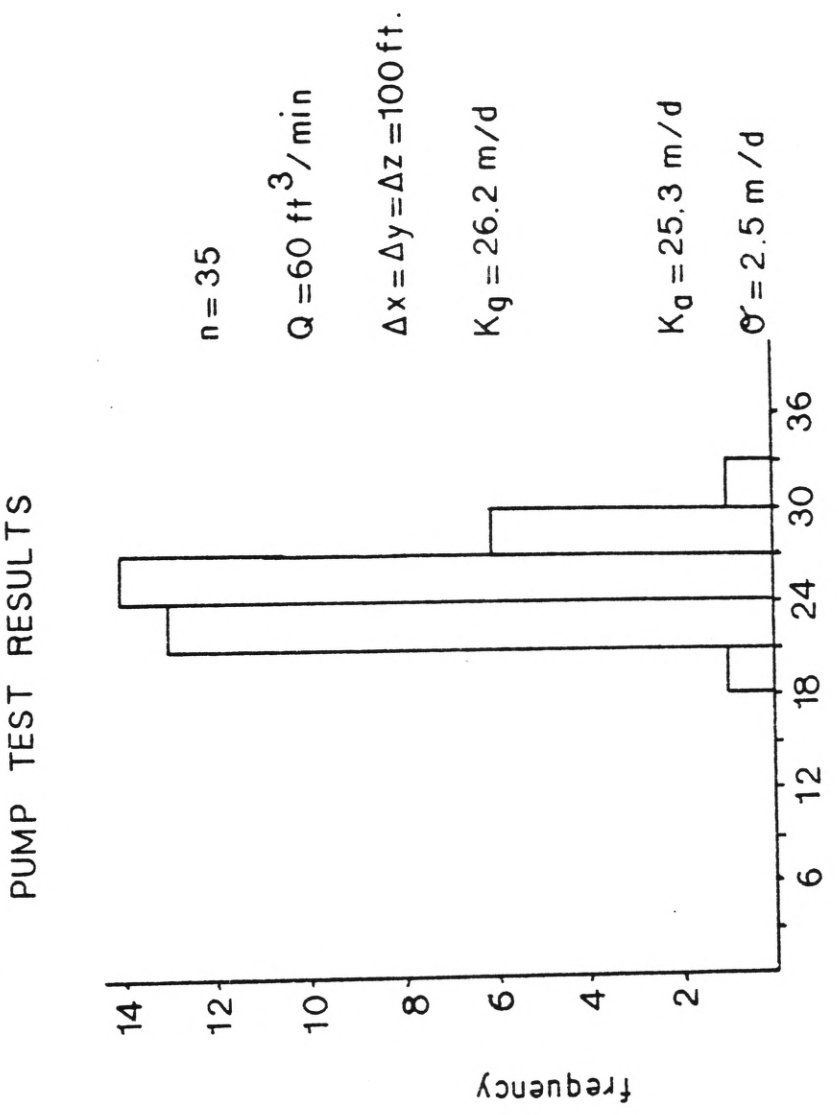

Figure 11. Three-dimensional pump test modeling results, delx and dely equal 100 feet.

geometric mean of the log-normal conductivity distribution. This time, however, the deviation (σ =2.5 meters/day) between conductivities determined from individual pump tests was negligible when one considers that conductivities in the log-normal distribution ranged over two orders of magnitude. The results of the 3-D pump test simulations support my second major assumption.

The decrease in standard deviation of conductivities observed when the grid spacing was decreased is interesting. With a large grid spacing the drawdown cone sampled a small number of the possible conductivity values in the system. Very different conductivity values could be obtained by rearranging the conductivity distribution. When the grid size was reduced the drawdown cone sampled far more conductivity values than before. The individual conductivities determined from the second model were more of an average of the conductivity distribution, therefore, rearranging the distribution caused less of a change in the conductivity value obtained from the pump test.

It is likely that the same phenomenon would be seen if the grid size was held constant and the pumping rate was increased. Increasing the pumping rate would be analogous to decreasing the grid size because the number of different conductivity values sampled would be increased. Therefore, the average conductivity value obtained from the pump test would be closer to the geometric mean of the conductivity distribution.

VI. NUMERICAL METHODS

The numerical techniques used to solve the groundwater flow equation (2) in the mass transport model was the method of Successive

Over Relaxation (SOR, Wang and Anderson, 1982). The algorithm for the SOR technique is documented in program MWALK which is listed in Appendix B. Flow was assumed to be in a steady state in the isotropic and nonhomogeneous system. The final form of equation (2) used in this study, therefore, is;

$$\partial/\partial x\left(T\,\partial h/\partial x\right)+\partial/\partial y\left(T\,\partial h/\partial y\right)+R=0 \qquad (16)$$

Where, T is transmissivity and all other terms have already been defined.

I tried using the Alternating Direction Implicit method (ADI, Prickett and Lonnquist, 1971) to solve (16), however, the heterogeneous nature of the system caused convergence problems. Freeze and Witherspoon (1967) used SOR successfully in their study of flow through heterogeneous porous media, also.

The finite difference grid used in this study is shown in Figure 12. The grid spacing is 272 feet in the x-direction and 360 feet in the y-direction. A total of 200 node points were used. For each node a finite difference equation of the following type was written.

```
H(I,J)=(B*T(I-1,J,2)*H(I-1,J) + B*T(I,J,2)*H(I+1,J)
       + A*T(I,J-1,1)*H(I,J-1) + A*T(I,J,1)*H(I,J+1)
       + Q(I,J))/(B*T(I,J,2) + B*T(I-1,J,2) + A*
       T(I,J,1) + A*T(I,J-1,1))
```

(17)

Where, A=dely/delx and B=delx/dely .

The boundary conditions on the mesh were determined after over-

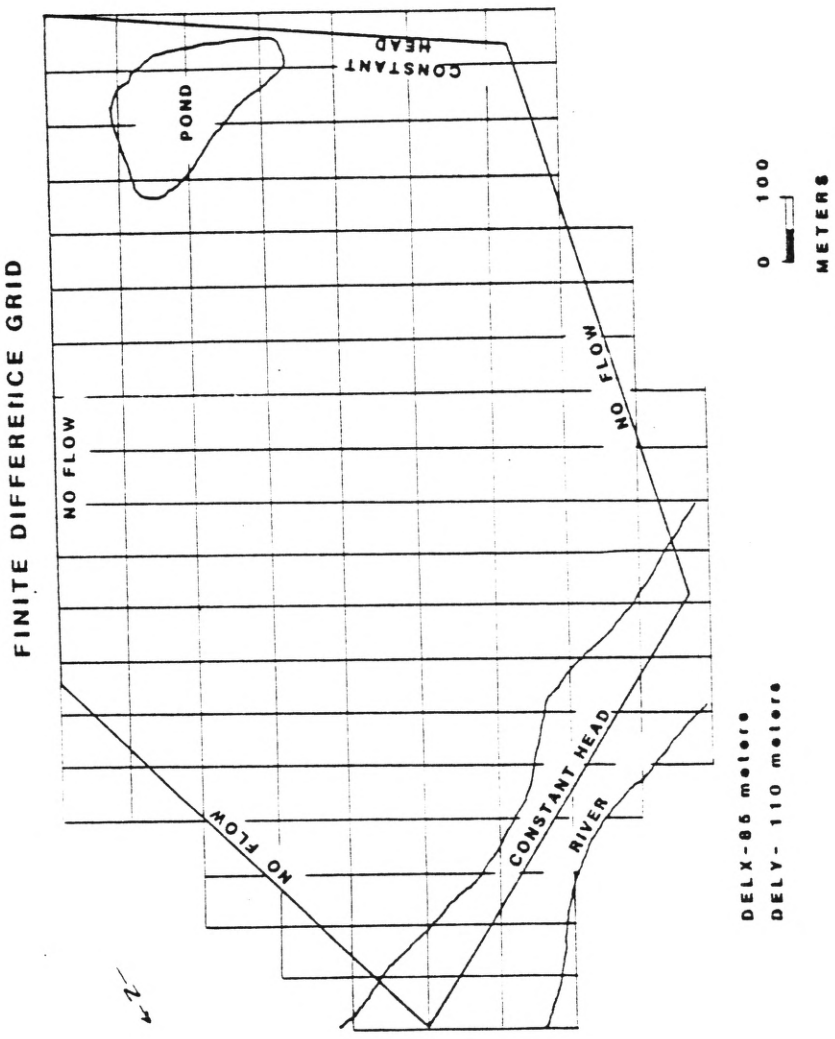

Figure 12. Finite difference grid used in the computer model.

laying the grid on Figure 7. Constant head boundaries correspond to the Canadian River and the 2741 foot water table contour. The remaining boundaries of the grid were taken as no-flow boundaries. The no-flow boundary to the east was aligned down the center of the Permian redbed outcrop. Because the redbeds are relatively impermeable (Geogulf, 1981), it is not likely that much water is flowing through these rocks and into the alluvium. Figures 13 and 14 are representative photographs of the Permian redbeds and alluvial sand bodies, respectively, at the site. The sand is medium grained, well sorted, and well rounded. The presence of a drainage ditch along the eastern boundary suggests that the alluvium may receive recharge in the area of the ditch. There was no means of determining the quantity of recharge from the ditch to the alluvium so the boundary was described as a no-flow boundary. The gradient is so small here (0.001) that the error introduced by assuming a no-flow boundary to the east is probably slight. The western no-flow boundary was aligned perpendicular to the water table contours.

Discretization of the 11 acre evaporation pond required three grid spaces. The rate of water leakage through the pond bottom was taken as 23,235 gallons/day (gpd). This was based on the pond's surface area, the height of water in the pond, depth to the water from the pond bottom, and the average soil permeability of the pond bottom as determined in laboratory falling-head permeameter tests (Fig. 15, Texas Dept. of Water Resources, Correspondence File). Leakage was represented by three recharge wells, each of which added 7745 gpd to the alluvium. It should be realized that water moving from the pond to the saturated zone flows

Figure 13. Photograph of the Permian redbeds south of highway 2277.

Figure 14. Photograph of an alluvial sand deposit along the Canadian River just east of the highway 2277 bridge.

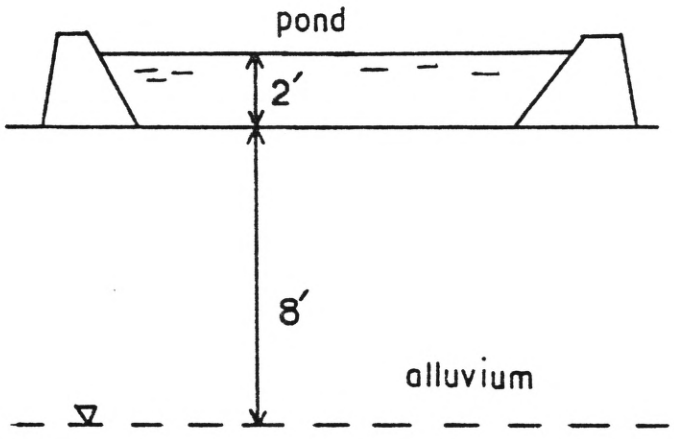

$Q = KiA$

$A = 11 \text{ acres} = 4.79 \times 10^5 \text{ ft}^2$

$i = 0.25$

$K = 0.21 \text{ gpd / ft}^2$

$Q = 23235 \text{ gpd}$

Figure 15. Sketch showing how the leakage rate from the pond was determined.

through an unsaturated zone of soil. The leakage rate used in the model is conservative, therefore, because the hydraulic gradient is equal to one for pure gravity flow.

The computer code written by Prickett and others (1981) was used for the mass transport model. The code is listed as program MWALK in Appendix B. The program combines a simple random walk technique for the dispersion part of transport, and the particle-in-a-cell technique for the convection portion of mass transport.

Random walk techniques take advantage of the equality in equation (12). The standard deviation of the particle distribution is directly proportional to the dispersivity. The dispersion component of transport is created in MWALK by:

$$\sqrt{2 \alpha_v DELT} * ANORM(0) \qquad (18)$$

where, DELT is the time step used in the simulation and ANORM(0) is a number between -6 and +6, drawn from a normal distribution of numbers having a standard deviation of one and a mean of zero. Equation (18) states that dispersion can transport mass up to six standard deviations away from the center of mass of the chloride distribution.

The particle-in-a-cell method moves each particle a distance v* DELT during every time step. The velocity in this equation is the average linear velocity determined from equation (1). Throughout this study porosity was assumed to be 30%. The total displacement for a given time

step for each particle is determined by:

$$\text{total displacement} = v * DELT + \left(\sqrt{2 d_\ell v * DELT} + \sqrt{2 d_t v DELT}\right) * ANORM(o) \quad (19)$$

where, all terms have already been defined.

The method used to produce the autocorrelated log-normal conductivity distributions was described by Smith and Freeze (1979). An autocorrelated log-normal conductivity distribution is one in which the hydraulic conductivity value at any point in a porous medium is dependent upon adjacent conductivity values. In a system that exhibits a large degree of autocorrelation, there is a tendency for zones of equal conductivity to be grouped together. For a system with a small degree of autocorrelation, zones of high conductivity are as likely to be situated near low conductivity as they are to other high conductivity zones. If K is log-normally distributed, Y=log(K) is normally distributed. Equation (20) defines the autocorrelation technique used by Smith and Freeze (1979) and this study.

$$Y_{ij} = \alpha_x \left(Y_{i-1,j} + Y_{i+1,j}\right) + \alpha_y \left(Y_{i,j-1} + Y_{i,j+1}\right) + \epsilon_{i,j} \quad (20)$$

Where, Y_{ij} is a random variable satisfying the autocorrelation relation

in equation (20), ϵ_{ij} is a normal, random distribution of numbers with a mean of zero and a standard deviation of one, α_x and α_y are auto-correlation parameters expressing the degree of spatial dependence of Y_{ij} on its neighboring values in the x- and y-directions, respectively, ($|\alpha| < 1$).

For a two-dimensional flow system such as that in Figure 12, the stochastic model for the entire set of p blocks (m rows x n columns) can be written as system of p linear equations (Smith and Freeze, 1979).

$$\{Y\} = [W]\{Y\} + \eta\{\epsilon\} \tag{21}$$

Where, $[W]$ is a pxp operator of scaled weights, w_{kl} (equation 22); and η is a multiplication factor used to obtain a Y_{ij} distribution with a specific standard deviation.

$$w_{k,\ell} = w^*_{k,\ell} / r \tag{22}$$

Where, w^*_{kl} equals α_x or α_y if blocks are adjacent in the x- or y-directions, respectively. The total number of adjacent blocks surrounding block k is equal to r. The solution to equation (21) is given by:

$$\{Y\} = ([I] - [W])^{-1} \cdot \eta\{\epsilon\} \tag{23}$$

where, $[I]$ is the identity matrix and all other terms were previously

defined.

The matrix in equation (23) was inverted using the Gauss-Jordan reduction method with partial pivoting (James et al., 1977). The solution yields the autocorrelated $\{Y\}$ vector which is normally distributed, $N(0, \sigma_y)$. The mean is then added, giving $N(\mu_y, \sigma_y)$. Finally, the log-normal hydraulic conductivity distribution is obtained by applying the exponential transformation (Smith and Freeze, 1979).

$$K_i = \exp(2.3026Y_i) \tag{24}$$

The conductivity values are then inserted into their appropriate grid spaces within the finite difference mesh.

The documentation for this algorithm is listed as program MK in Appendix B.

The statistical program MSTAT (Appendix B) was written in order to calculate the mean and standard deviation (based on 20 runs using a different K distribution each time) of hydraulic conductivity and (Cl^-) at each node in the system.

Figure 16 illustrates a flow chart describing the sequence in which the various programs were run in order to produce a complete simulation.

VII. RESULTS

A. Deterministic Model

The system was first modeled deterministically. The head distribution calculated using the average hydraulic conductivity (5.2 meters/day) obtained from the pump test is shown in Figure 17. There was good

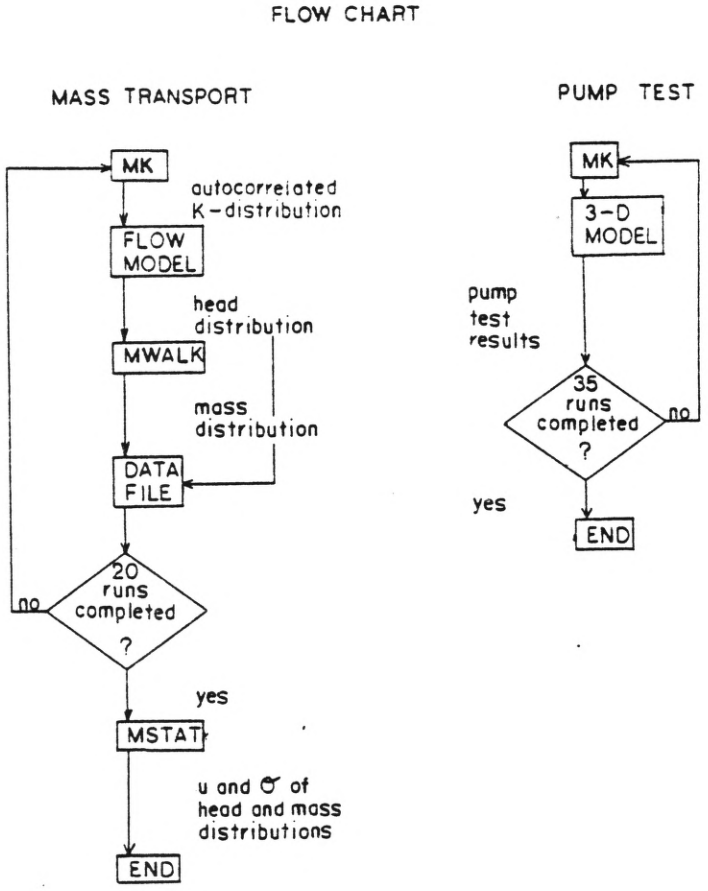

Figure 16. Flow chart illustrating sequence in which computer programs were executed in order to produce a complete stochastic simulation.

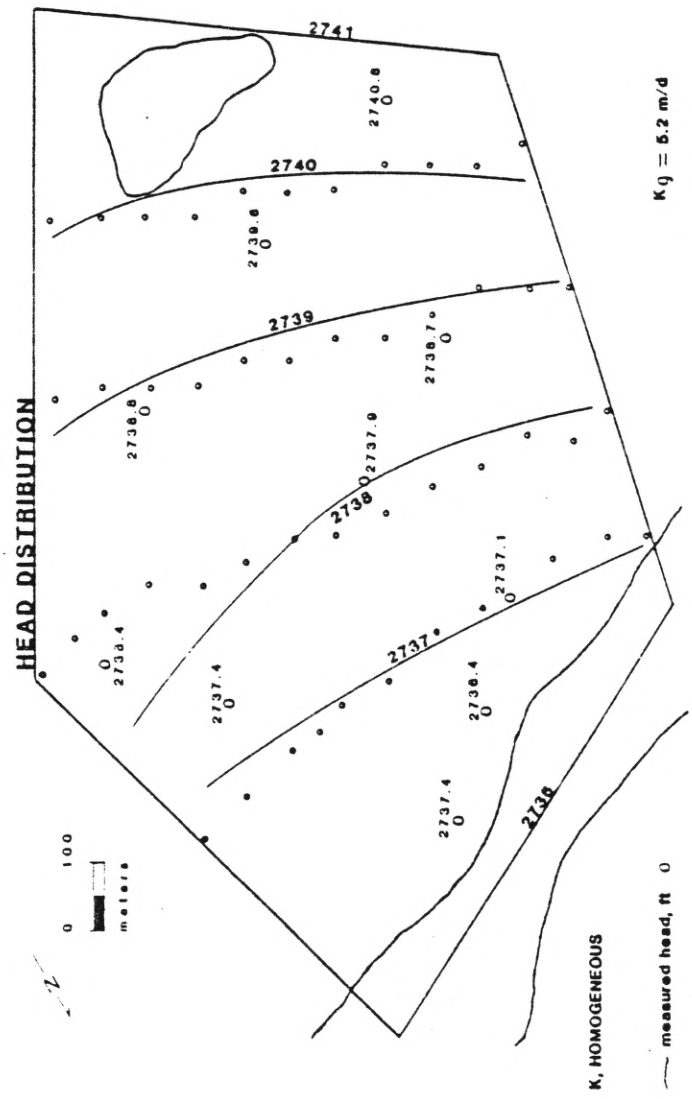

Figure 17. Head distribution, homogeneous K distribution.

agreement between the observed and modeled head values except along the eastern half of the 2738 foot water level contour. I considered the deviation along the eastern boundary acceptable as the hydraulic gradient of the system was small (0.001). The distribution of measured heads along the eastern no-flow boundary indicates that the alluvium may have been receiving recharge at this boundary from the bedrock outcrop to the east (Fig. 7). There is also a well developed drainage ditch paralleling highway 2277. The alluvium could have received recharge through the ditch. In any event it must be recognized that the "measured" potentiometric surface is based on only eleven data points. Many other plausible water table surfaces could have been created to fit the given water level data.

There was no noticeable bending of the water level contours around the pond, indicating recharge, in either the measured or calculated head data. In the case of the measured head data, the quantity of water level data close to the pond was insufficient to delineate these trends in gradient. The grid spacing was probably too coarse in the case of the calculated data.

The chloride distribution obtained with equation (15) is shown in Figure 18. The wells were sampled for dissolved chloride at four times in 1981 and 1982 (Table I). The concentrations assigned to each well in Figure 18 represent the average concentration of the four measurements. The time available for transport was 41 years (1940-81). It should be realized that the chloride measured at the wells represented a component from the pond and a component initially present in the system. The ambient chloride concentration measured in the groundwater was about 600 mg/l (Geogulf, 1981). This was measured in a well nearly 1000 feet

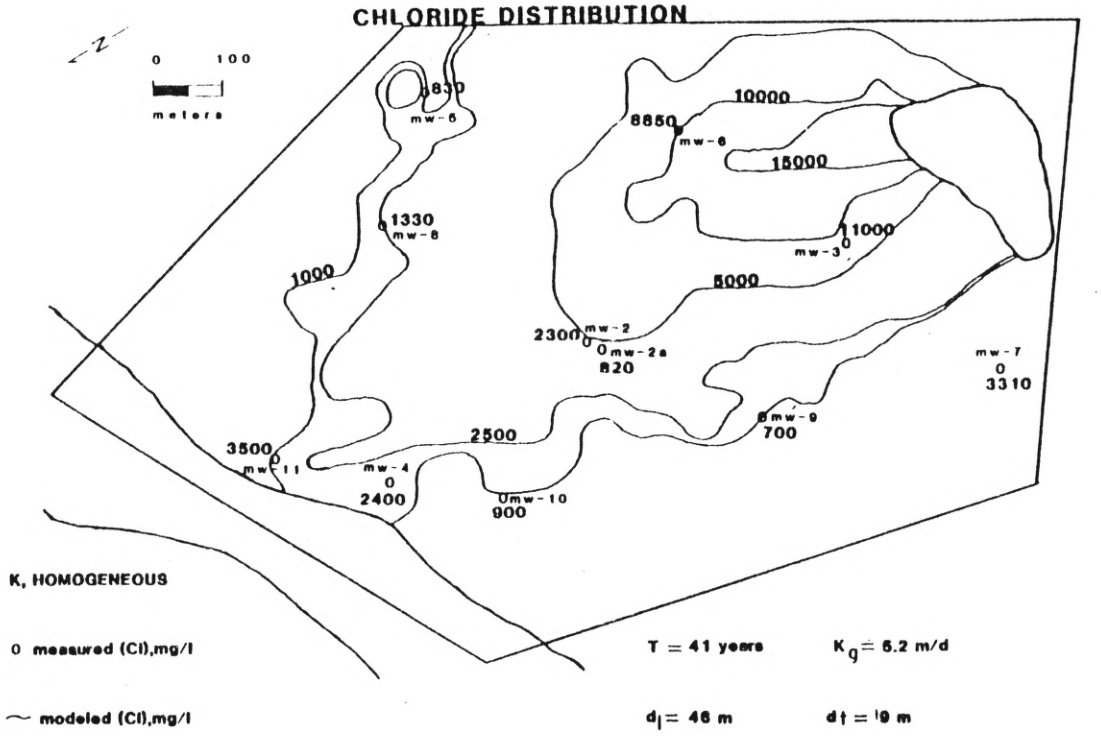

Figure 18. Chloride distribution, homogeneous K distribution.

TABLE I. Measured (Cl^-) in mg/l for the period 1981-82.

monitor well	May 1981	June 1982	Sept. 1982	Nov. 1982
1	600	600	615	670
2	2300	2400	1900	2500
2A	820	800	800	1000
3	11000	9500	8300	9700
4	2400	2500	2100	2500
5	830	800	700	1000
6	8850	8900	9300	8100
7	3310	3400	3400	3100
8	1330	1400	1300	1300
9	700	600	700	800
10	900	800	900	1000
11	3500	3400	3900	3300
up river		1400	1800	1700
down river		1700	1800	2000

up-gradient of the pond (MW-1, Fig. 7)(Texas Dept. of Water Resources).

As was stated in the geology section, the study area is located in a major salt dissolution zone. Chloride concentrations in groundwater issuing from springs within these salt dissolution areas can be orders of magnitude greater than the 600 mg/l measured at MW-1 (Richter, 1983). Therefore, it is possible that the ambient chloride concentration in the groundwater is greater than 600 mg/l. In addition, the ambient (Cl^-) may be spatially variable (see Richter's Tables A-1 and A-2), not constant at 600 mg/l. There was no evidence of saline springs or seeps on the site itself. Furthermore, the average (Cl^-) in the Canadian River, as measured at the highway 152 bridge, was about 1,800 mg/l (Table I). Both of these facts suggest that the ambient (Cl^-) was probably not unusually high at my study area. More data would be required to delineate the spatial variability of dissolved chloride at the site. In summary, the 600 mg/l used as the ambient (Cl^-) in this study is a best estimate based upon the available data.

The computer generated distributions reflect both the chloride from the pond and that originally present in the system. This was done by adding 600 mg/l chloride to the chloride concentration calculated at each node to have been contributed by the pond. The rate at which dissolved chloride was added by the pond was calculated on the basis of the leakage rate from the pond (23,235 gpd) and the chloride concentration in the pond (25,000 mg/l)(Texas Dept. Water Resources). Chloride, therefore, was added at the rate of 2.2×10^3 kg/day.

Longitudinal and transverse dispersivities of 46 meters and 9 meters, respectively, were required to produce the match in Figure 18.

The dispersivities were adjusted until the modeled chloride distribution approximated the measured distribution. The marked difference between chloride measured at MW-2 and MW-2A is interesting. Well 2 was screened from 50 to 90 feet beneath the surface while well 2A was screened in the upper 20 feet of the aquifer. The wells are only about 65 feet apart. This difference in measure chloride could be due to density stratification of the groundwater in the alluvium. It might also be from preferred movement of groundwater along a high conductivity zone which was intersected by MW-2. In either case a three-dimensional or profile-oriented model would be required to simulate this phenomenon.

The chloride concentrations measured at wells 3, 7, and 11 (see Figure 18) could not be reproduced adequately by the deterministic model. However, wells 3 and 11 do lie close to their appropriate concentration fields. An increase in the longitudinal dispersivity could have provided a better match at these wells at the price of reducing the quality of the match at some other wells. For examples notice wells 2, 6, and 8. Increasing the longitudinal dispersivity causes the isochors to be moved further down-gradient (equation 19). Such is the nature of the deterministic modeling technique. The anomalously high dissolved chloride at wells 7 and 11 are hard to explain with the limited data available to me. In both cases preferred groundwater flow along high conductivity zones intersected by these wells may be responsible for the extra dissolved chloride at the wells. Greater leakage than simulated from the western end of the pond may have increased flow towards MW-7, also.

Based on the average hydraulic gradient and hydraulic conductivity of the system the dissolved chloride plume advanced about 10 meters/year.

Travelling at this velocity, neglecting dispersion, the plume would have advanced only half the distance to the river in the time available for transport (41 years). However, due to dispersion of the chloride the 1,000 mg/l isochore, at least, has reached the river.

B. Stochastic (Random) Model

The system was next modeled stochastically using a random log-normal hydraulic conductivity distribution. A random distribution is indicated by alpha equal to zero. This means that there is no spatial dependence between adjacent conductivity values. In all the stochastic models statistical isotropy ($\alpha_x = \alpha_y$)(Smith and Freeze, 1979), was assumed. However, anisotropy was introduced by the grid spacing as chosen for the finite difference grid (Fig. 12). This was necessitated by the nature of the numerical technique used to produce the hydraulic conductivity distributions used in the stochastic models. The technique involved inverting a p x p matrix, $[W]$. Using a grid spacing where delx =dely would have created a prohibitively large matrix in terms of computer time required to invert $[W]$.

The anisotropy produced by the unequal grid spacing is analogous to creating constant conductivity lenses oriented parallel to the y-direction. The y-direction is subparallel to the river (Fig. 12), however, along which river-deposited lenses of sand and gravel would be oriented (Reading, 1978, p. 21). The anisotropy in the conductivity distribution, therefore, generally reflects the macroscopic structure of the braided stream deposit. That is, high conductivity lenses in the stochastic model represent sand and gravel in the braided stream

deposit. Figure 19 is a photograph of the channel of the Canadian River taken from the highway 2277 bridge. The photograph shows a channel sand deposit (on the right) located adjacent to a deposit of clayey silt. These deposits are oriented parallel to the river channel.

The mean head distribution is shown in Figure 20. The match between observed and calculated heads is good along the 2737 foot water table contour and western portions of the remaining contours. However, there was a good deal of deviation along the eastern boundary of the model. This may be due to poorly prescribed boundary conditions to the east and/or insufficient sampling of the possible conductivity distributions in the system.

Theoretically, the flux calculated at any node in the deterministic model should equal the average flux at that same node in the stochastic model if the geometric mean of the hydraulic conductivity distribution is the effective conductivity of the system (Smith and Freeze, 1979). This should be reflected by the match between observed and calculated hydraulic heads. Since it is assumed that the geometric mean of the conductivity distribution is the effective conductivity of the system (see Section V), the match between observed and calculated heads should indicate whether the sample of hydraulic conductivities had been sufficiently large to produce this equality of fluxes at each node. The match was relatively good except along the east boundary. This suggests that 20 conductivity distributions might have been enough, but that the boundary conditions specified along the eastern boundary were not realistic.

Figure 19. Photograph of the Canadian River from the highway 2277 bridge looking west. The photograph represents approximately a 30 foot cross section of the river.

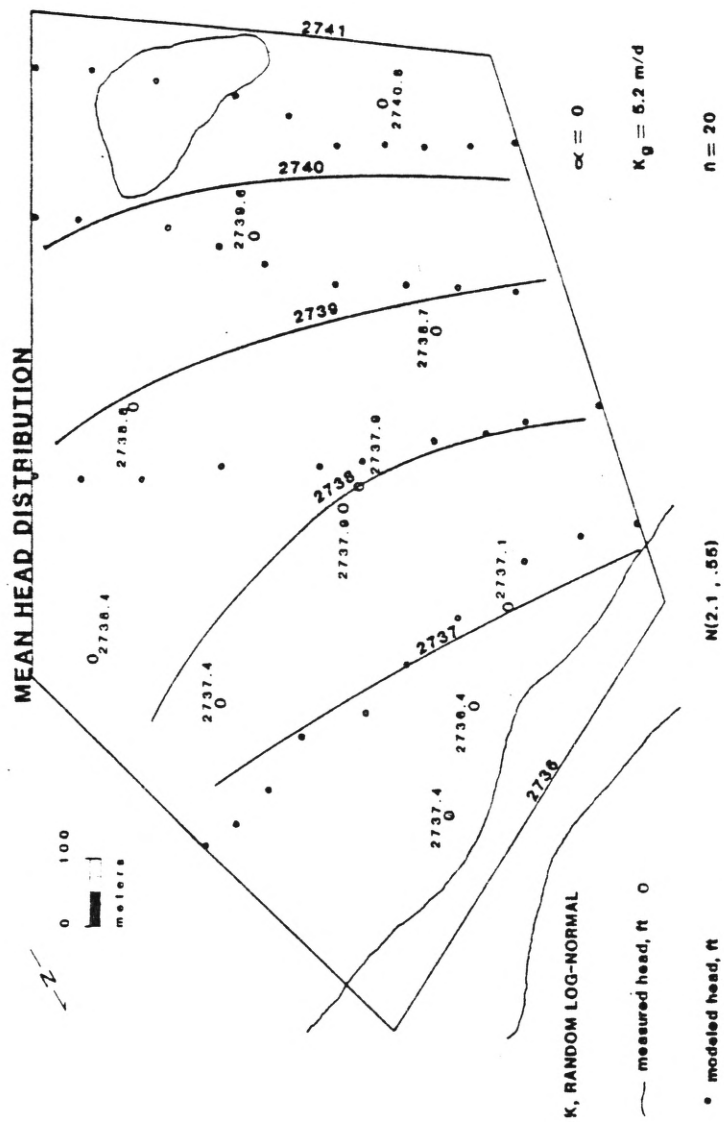

Figure 20. Mean hydraulic head distribution for the random log-normal hydraulic conductivity distribution.

Another interpretation is that where boundary conditions were accurately described, the system was less sensitive to the number of hydraulic conductivity distributions examined. Along the west boundary, therefore, a good match was observed. On the other hand, the no-flow boundary to the east may have accentuated the potentially insufficient averaging provided by the small sample size of the conductivity distribution. This would be reflected by the large deviation in observed and calculated hydraulic heads to the east in the study area.

The standard deviation is a measure of the uncertainty in the calculated mean head distribution. The standard deviation in heads for the random system is shown in Figure 21. Uncertainty is zero at the two constant head boundaries and generally increases away from these boundaries. Uncertainty is also high under zones of high hydraulic gradient such as beneath the pond. The calculated hydraulic gradient is greater along the western boundary than along the eastern boundary (Fig. 20). This is reflected in Figure 21 by the larger uncertainty in mean heads to the west in comparison to the east. The greatest uncertainty in head (0.25 feet) is only 5.0% of the total head drop across the flow system. This is a small degree of uncertainty.

The mean dissolved chloride distribution produced by the random log-normal conductivity distribution is shown in Figure 22. Initially, I thought that the amount of spreading would be much greater for the random system than for the homogeneous system described in Section VII.A. However, using the same dispersivities as in the deterministic model produced less longitudinal and more transverse spreading of the dis-

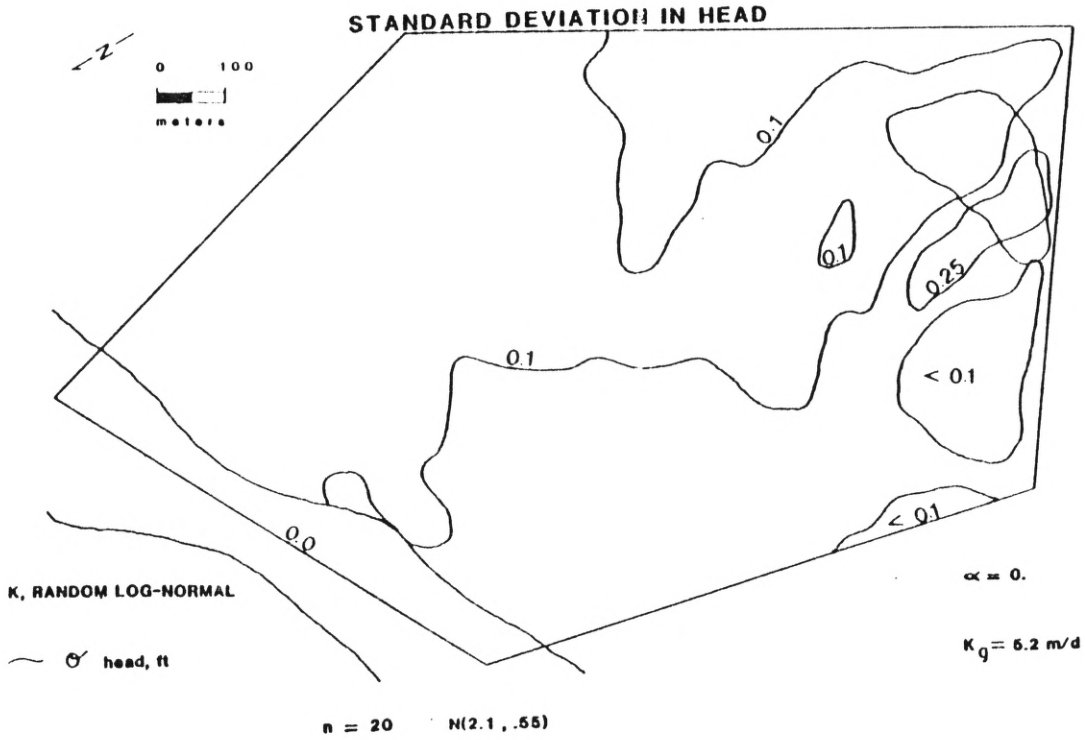

Figure 21. Standard deviation in hydraulic head for the random log-normal hydraulic conductivity distribution.

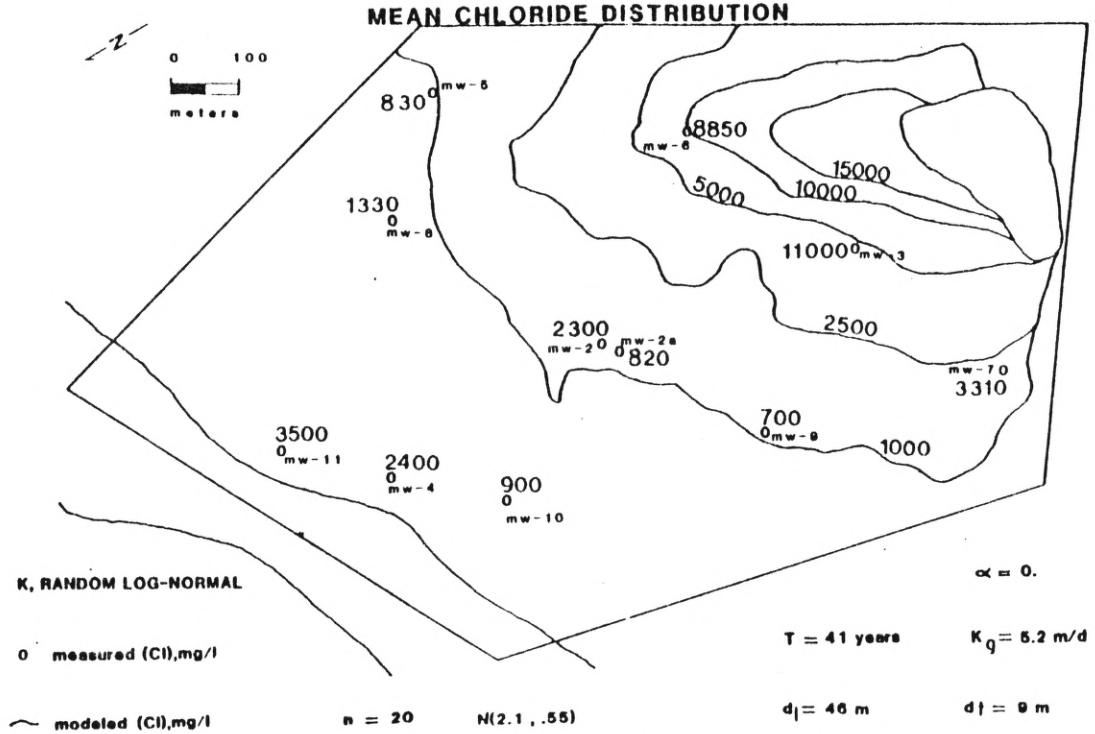

Figure 22. Mean chloride distribution for the random log-normal hydraulic conductivity distribution.

solved chloride. The increase in transverse spreading caused MW-7 to fall closer to its appropriate concentration field than it did in the homogeneous case. However, the decrease in longitudinal dispersion left MW-4, 8, and 11 further from their appropriate concentration fields.

Figure 23 illustrates why the random log-normal hydraulic conductivity distribution produced less longitudinal and more transverse spreading of the dissolved chloride than did the homogeneous system. The random log-normal distribution of conductivities in Figure 23 represents only one of an infinite number of possible conductivity distributions having the same mean and standard deviation. The zones of highest conductivity are represented by the dots while the lowest conductivity zones are blank. There is little or no interconnection between high conductivity zones in this example, therefore, the groundwater has no direct path to follow. Rather, the flowlines follow a very tortuous path that is influenced by the randomly spaced, isolated high conductivity zones. I believe the irregular flowpaths were responsible for the decreased longitudinal and increased transverse spread in dissolved chloride. The effectiveness of high conductivity zones in capturing groundwater flow was demonstrated by Freeze and Witherspoon (1967). They used a numerical model to simulate regional groundwater flow patterns. It was found that the distribution of high conductivity zones influenced such things as the size and location of recharge and discharge areas; and the quantities of flow passing through different zones within the system.

Uncertainty in the mean chloride distribution is indicated by the standard deviation in dissolved chloride. Figure 24 shows the pattern

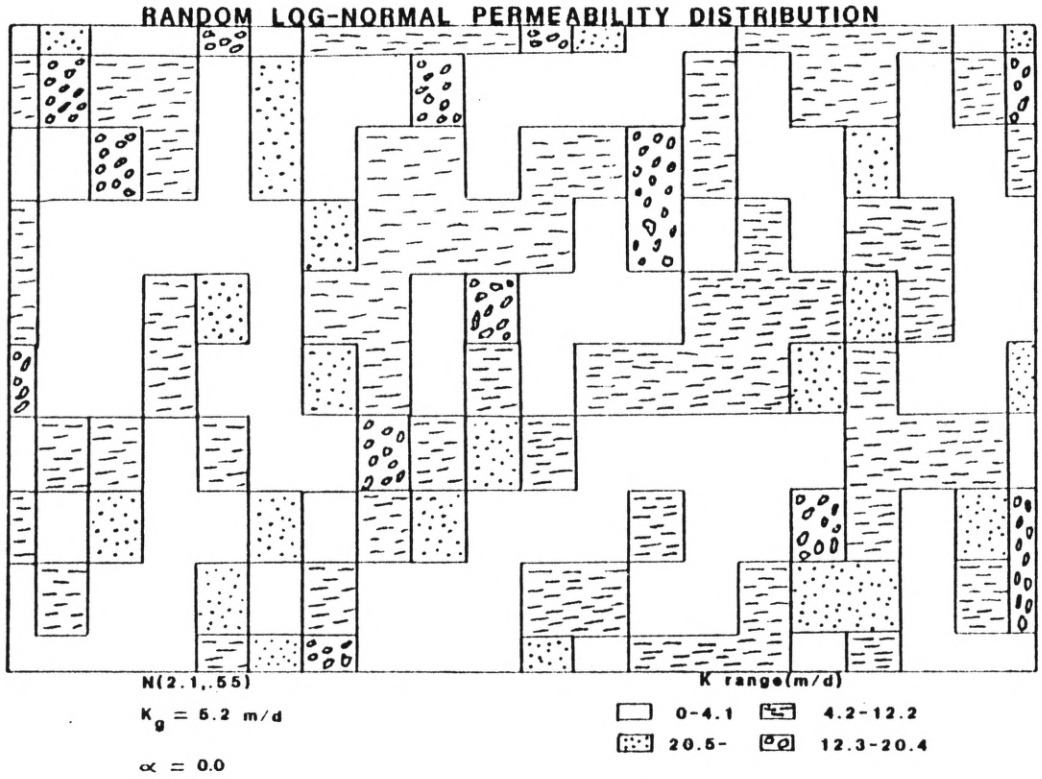

Figure 23. Example of a random log-normal hydraulic conductivity distribution produced by program MK.

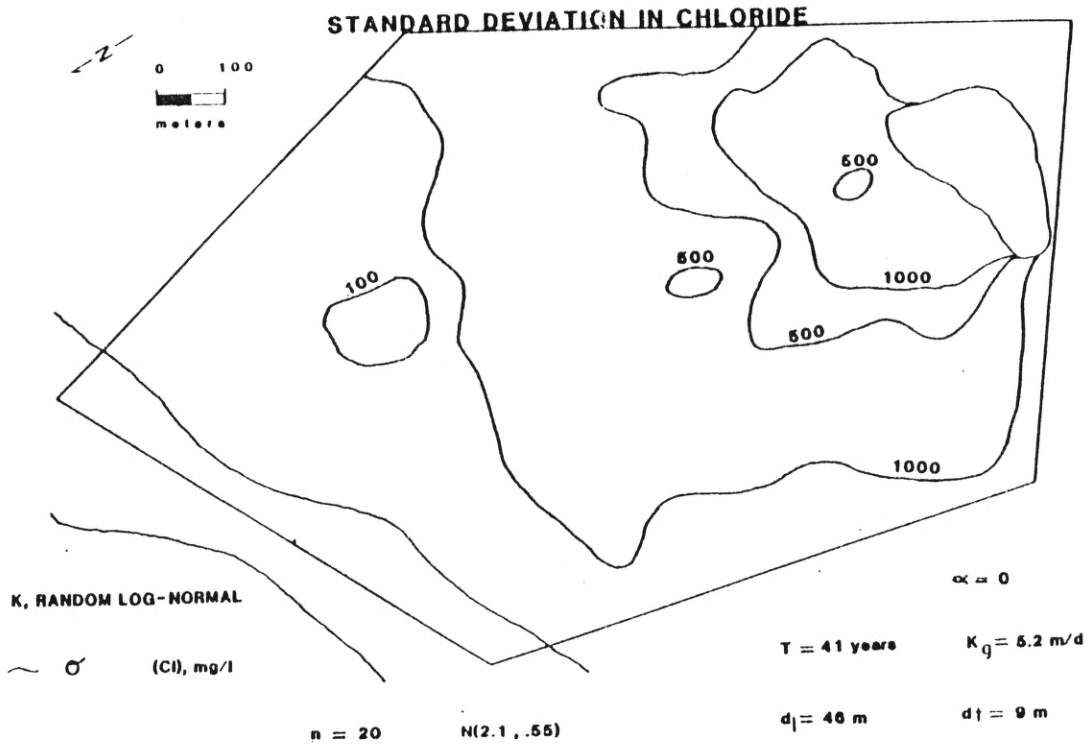

Figure 24. Standard deviation in chloride produced by the random log-normal hydraulic conductivity distribution.

of standard deviations in dissolved chloride for the random log-normal hydraulic conductivity distribution. The uncertainty in dissolved chloride decreased away from the source of chloride, the pond. This decrease in uncertainty in mean chloride away from the pond simply reflects the decrease in chloride concentrations down-gradient from the source (Fig. 22). That is, dissolved chloride varied less because there was less dissolved chloride to begin with. It must be pointed out that the uncertainty in (Cl^-) shown in Figure 24 is based upon the computer-generated chloride distribution shown in Figure 22. That chloride distribution did not match the observed distribution at the river. If the modeled chloride distribution had matched the measured chloride distribution at the river, the uncertainty in chloride would have been greater than shown in Figure 24. Again, this is because larger (Cl^-) allows greater deviations in dissolved chloride away from the mean.

C. Stochastic (Autocorrelated) Model

The system was again modeled stochastically, but this time an autocorrelated log-normal conductivity distribution was used. This is indicated by alpha equal to 0.7, which means strong spatial dependence between adjacent conductivity values. The distribution of calculated and observed hydraulic heads is shown in Figure 25. The calculated mean head distribution matched the observed distribution better than did that of the random system (Fig. 20). There was excellent agreement along the 2737 foot water table contour and western halves of the remaining contours. The eastern portions of the 2739 foot and 2740 foot contours are much closer to the observed contours than they were for the system with

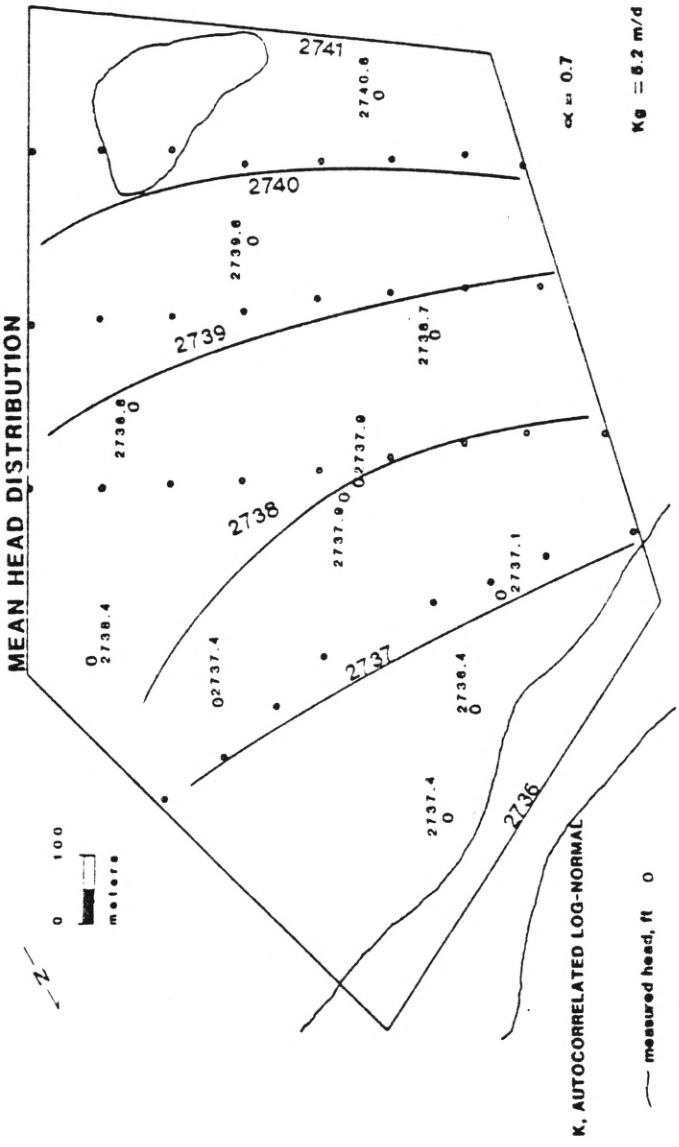

Figure 25. Mean head distribution produced by the autocorrelated log-normal hydraulic conductivity distribution, alpha=0.7.

the random log-normal conductivity distribution. The effect of the no-flow boundary to the east is still evident. All of the calculated mean head contours must intersect this boundary at right angles in the flow model even though the observed heads bend toward the river.

The standard deviation in heads for the autocorrelated log-normal conductivity distributions is shown in Figure 26. The patterns are similar to those in the random system (Fig. 21). However, the magnitude of uncertainties is greater for the autocorrelated system. The greatest uncertainty in hydraulic head (0.50 feet) is 10% of the total head drop across the flow system. This increase in uncertainty in hydraulic heads with increased autocorrelation of hydraulic conductivities was also observed by Smith and Freeze (1979), Freeze (1975), and various other researchers.

Smith and Freeze (1979)

> consider the case where a series of high or low conductivity values (relative to the mean conductivity of the statistically homogeneous medium) are inserted into adjacent blocks. The hydraulic head solution for this conductivity realization can then move further away from its mean hydraulic head solution for that region within the flow domain. For large integral scales it is more probable that the conductivity realizations will exhibit such behavior. On averaging over the series of runs, this alignment of like conductivity values within each realization tends to increas the standard deviation in the hydraulic head distribution at any point within the flow domain.

Increasing the integral scale produces the same effect as increasing alpha. A statistically homogeneous system is one in which the conductivity distribution is monomodal.

Not only does the uncertainty in mean head change as the degree of autocorrelation changes, but it also changes when you compare one-,

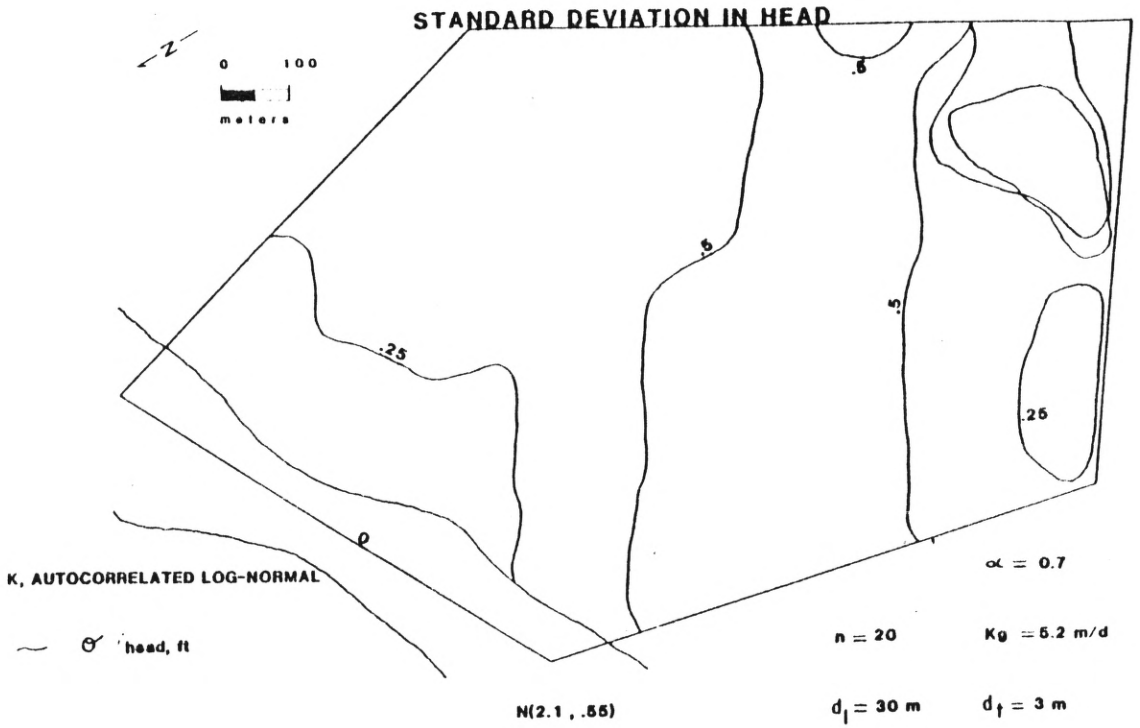

Figure 26. Standard deviation in head produced by the autocorrelated log-normal hydraulic conductivity distribution, alpha=0.7.

two-, and three-dimensional systems (Smith and Freeze, 1979). In a one-dimensional flow system flow cannot be routed around low conductivity inclusions so that their position in the flow system will control the hydraulic head values all along the flowpath. The effect of low conductivity zones is localized in a two-dimensional system because flow can move laterally around the low conductivity zones. Low conductivity zones are the least effective in controlling hydraulic head distributions in a three-dimensional system because flow can be rerouted laterally and vertically around low conductivity zones. Smith and Freeze (1979) stated that uncertainties in mean hydraulic head were cut in half in going from a one- to a two-dimensional flow system. They reported that Gelhar found an order of magnitude difference in uncertainties in hydraulic head between one- and two-dimensional systems. Bakr and others (1978) saw an order of magnitude reduction in the standard deviation in hydraulic heads in going from a one- to a three-dimensional flow system.

The mean dissolved chloride distribution produced with alpha equal to 0.7 is shown in Figure 27. Even with the longitudinal dispersivity reduced to 30 meters from 46 meters used in the previous examples, there was a marked increase in the longitudinal spread of dissolved chloride over that produced by the system having a random log-normal conductivity distribution. More transverse dispersion of chloride was also produced by the autocorrelated system than for either of the previously described systems containing homogeneous and random conductivity distributions. The significant reduction in longitudinal dispersivity along with the large amount of spreading of dissolved chloride indicates that large-scale mixing is produced by autocorrelated log-normal hydraulic conduc-

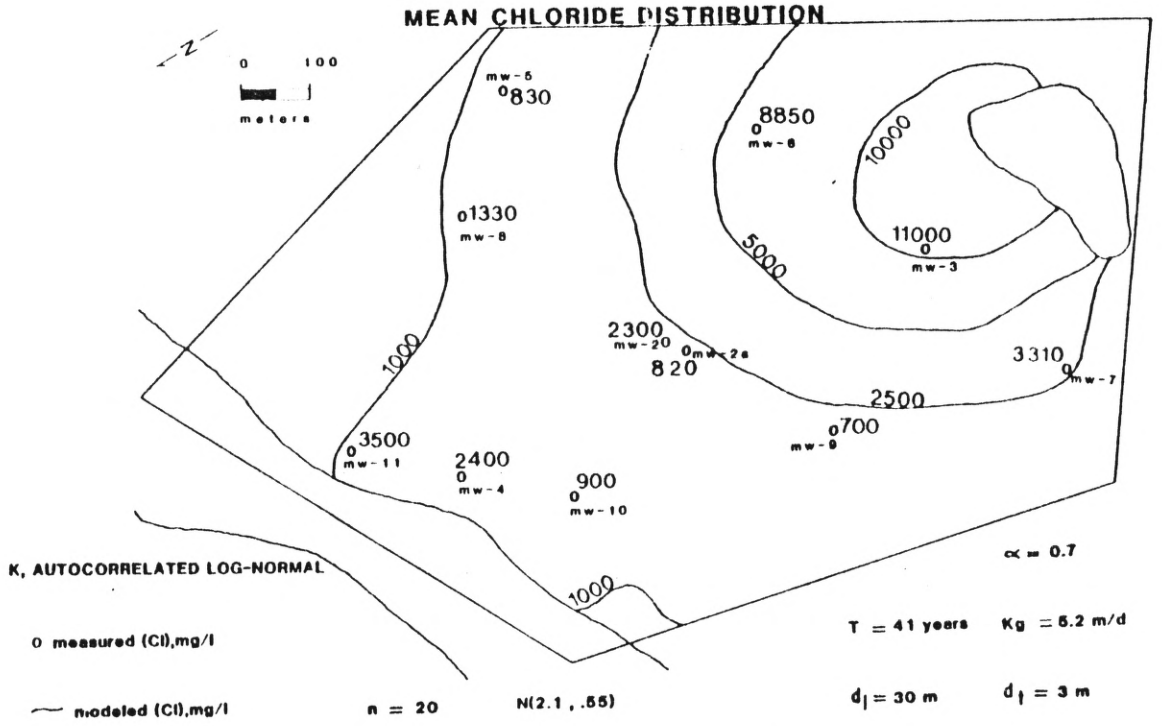

Figure 27. Mean chloride distribution produced by the autocorrelated log-normal hydraulic conductivity distribution, alpha=0.7.

tivity distributions.

Geogulf (1981) used a one-dimensional analytical model to simulate the chloride movement at the study site. They had to use a longitudinal dispersivity of 111 meters in order to obtain an acceptable match between observed and modeled chloride distributions. The two-dimensional model used in this study that contained a homogeneous conductivity distribution required a longitudinal dispersivity of 46 meters. This was reduced even further to a longitudinal dispersivity of 30 meters for the stochastic model in which alpha equalled 0.7. It is very likely that modeling the system stochastically in three dimensions would reduce the longitudinal dispersivity even more. If the amount of reduction in uncertainty in hydraulic heads produced in going from one-, to two-, to three-dimensions is any indication, the dispersivity might be reduced by an order of magnitude. This would be due to increased divergence of flowlines around low conductivity zones in the three-dimensional model and, therefore, more large-scale mixing. If all of the significant scales of heterogeneity were accounted for in the three-dimensional model, no dispersivity at all would be required in the computer model. Only advection and diffusional transport would have to be modeled. Both of these transport mechanisms are adequately described mathematically.

Unlike the dissolved chloride distributions exhibited in Figures 18 and 22, the chloride distribution produced with alpha equal to 0.7 did account for the measured chloride in MW-3 and 7. However, MW-8, 9, and 10 have dissolved chloride concentrations less than the field in which they are located. All of these wells are screened in the upper fifteen feet

of the aquifer, therefore, the inexactness of the match may be due to insufficient sampling of the dissolved chloride in the groundwater at these wells. In general, the amount of longitudinal and transverse dispersion of the chloride is greater in the system with the autocorrelated conductivity distribution than it was in either of the previous two examples. It was also the only example not to develop a 15,000 mg/l isochore.

The increased longitudinal dispersion of dissolved chloride observed in the autocorrelated system over that produced in the other examples is explained in Figure 28. As with Figure 23, this is only one of an infinite number of possible distributions having the same mean and standard deviation. There is a good deal of interconnection between high conductivity zones in the autocorrelated distribution. In other words, the groundwater has direct paths to follow down-gradient. These interconnected high conductivity zones are analogous to sand and gravel lenses commonly observed in alluvial sediments (Bridge and Leeder, 1979).

The influence of interconnected high conductivity zones on groundwater chemistry is illustrated in the Catahoula Formation of the Texas Coastal Plain (Galloway and Kaiser, 1980). The Catahoula Formation consists of two major ancient fluvial systems. The Gueydan fluvial system is centered in the Rio Grande Embayment, and the Chita-Corrigan fluvial system is centered in the Houston Embayment (Galloway and Kaiser, 1980). Net sand and chlorinity maps show that the sand-rich axes of the fluvial systems display a broad lobe of very fresh, low chloride water. This indicates a well flushed system. The margin of the lobes are indented where high-chloride waters occupy muddier interchannel facies

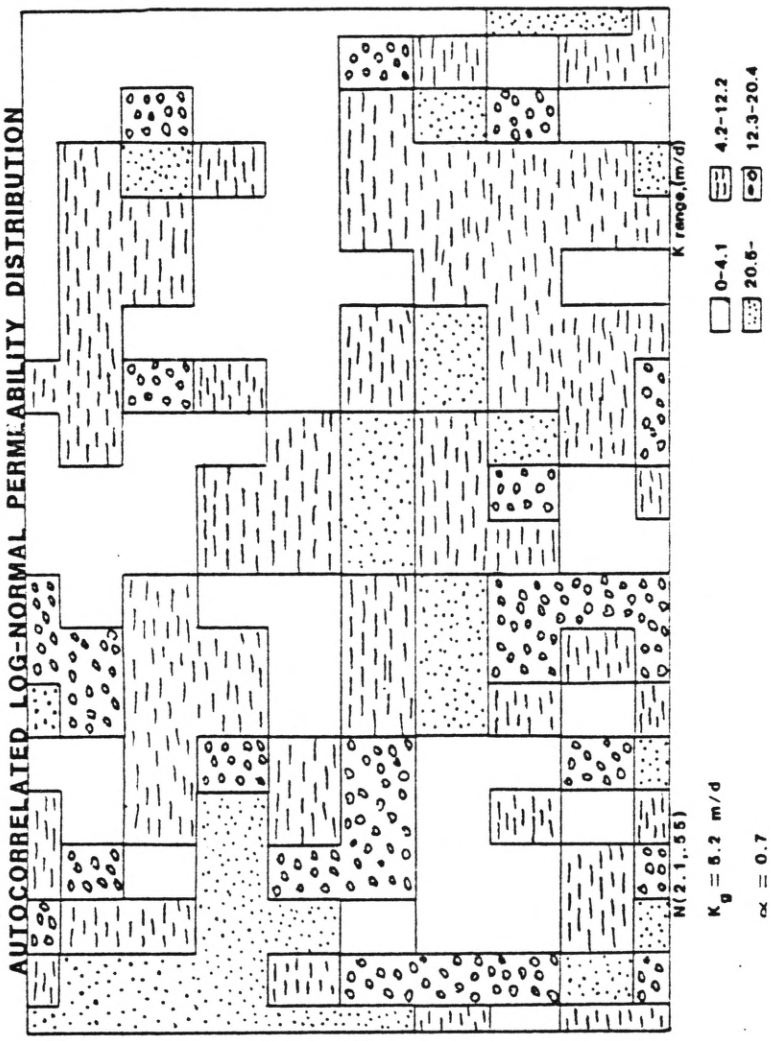

Figure 28. Example of an autocorrelated log-normal hydraulic conductivity distribution produced by program MK.

(Galloway and Kaiser, 1980). The roll-type uranium deposits within the Catahoula are situated in the sand-rich channel and crevasse splay deposits. The mechanisms of uranium transport are similar to those for (Cl^-) transportation, therefore, the presence of uranium deposits in the high conductivity zones indicates that groundwater flow is concentrated within these zones.

The standard deviation of dissolved chloride is shown in Figure 29. As with the system containing a random distribution of conductivities, uncertainty in chloride decreased away from the source. Further from the source there is less mass available to deviate from the mean concentration. The magnitude of the uncertainties is larger for the autocorrelated system than it was for the random system. This is due to the nature of transport in the two systems. Mass is transported further in the system containing an autocorrelated log-normal conductivity distribution. At any given point, therefore, the amount of dissolved chloride available to deviate from the mean concentration is greater for the autocorrelated system than for the random system.

The distributions of hydraulic head and chloride produced when alpha equalled 0.3 and 0.5 were examined, also. The results of these simulations are shown in Figures 30-37. The match obtained between observed and modeled hydraulic heads was better when alpha equalled 0.3 than it was for alpha equal to 0.5 (Figures 30 and 34). Generally, there was no direct relationship between the quality of the match in heads and the degree of autocorrelation in hydraulic conductivities. The best match was obtained with alpha equal to 0.7, and the worst match was produced

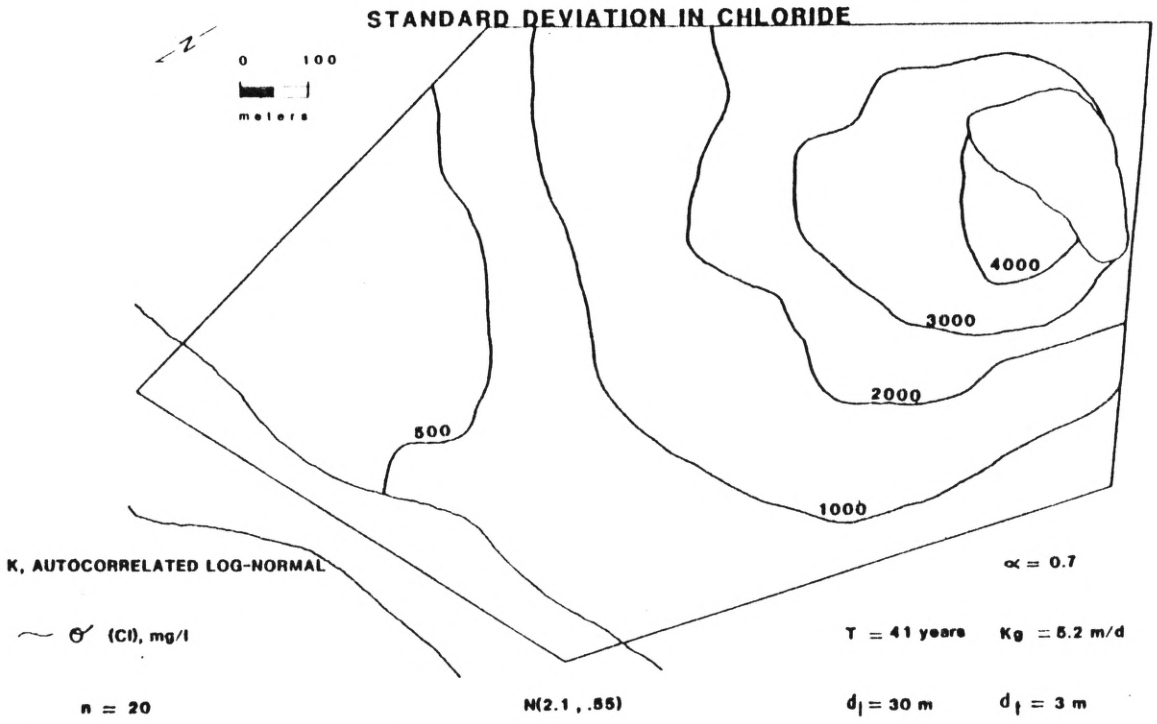

Figure 29. Standard deviation in chloride produced by the autocorrelated log-normal hydraulic conductivity distribution, alpha=0.7.

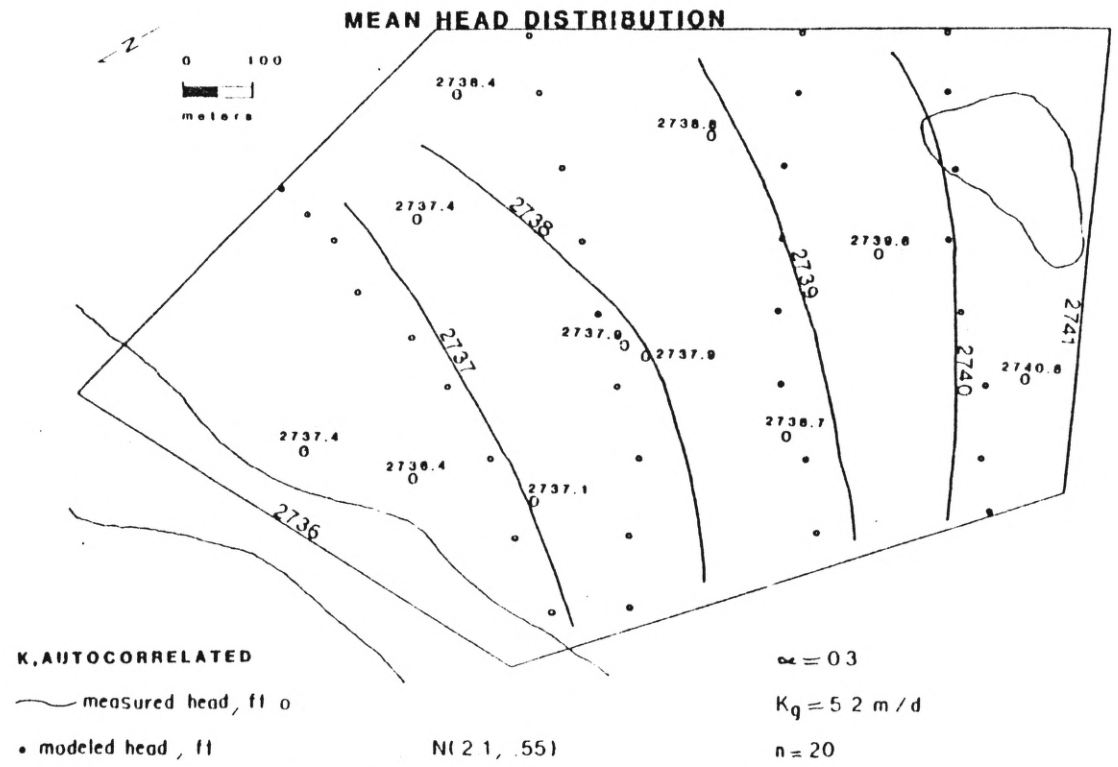

Figure 30. Mean hydraulic head distribution produced by the autocorrelated log-normal hydraulic conductivity distribution, alpha=0.3.

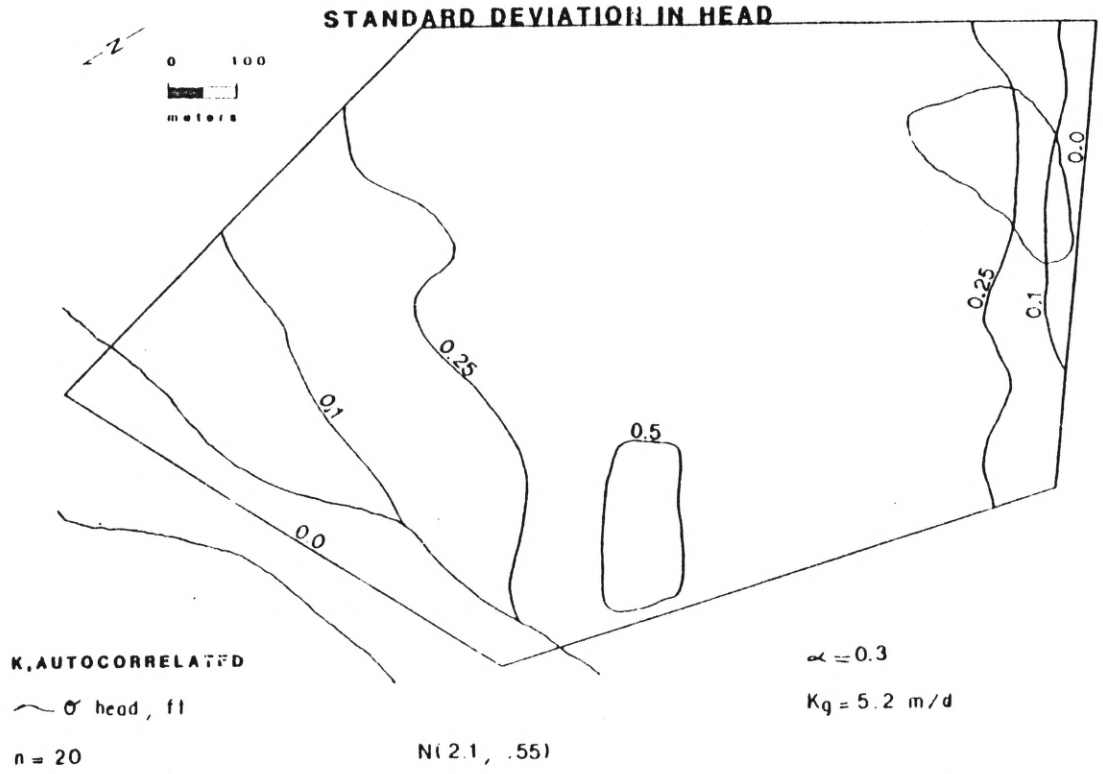

Figure 31. Standard deviation in hydraulic head produced by the autocorrelated log-normal hydraulic conductivity distribution, alpha=0.3.

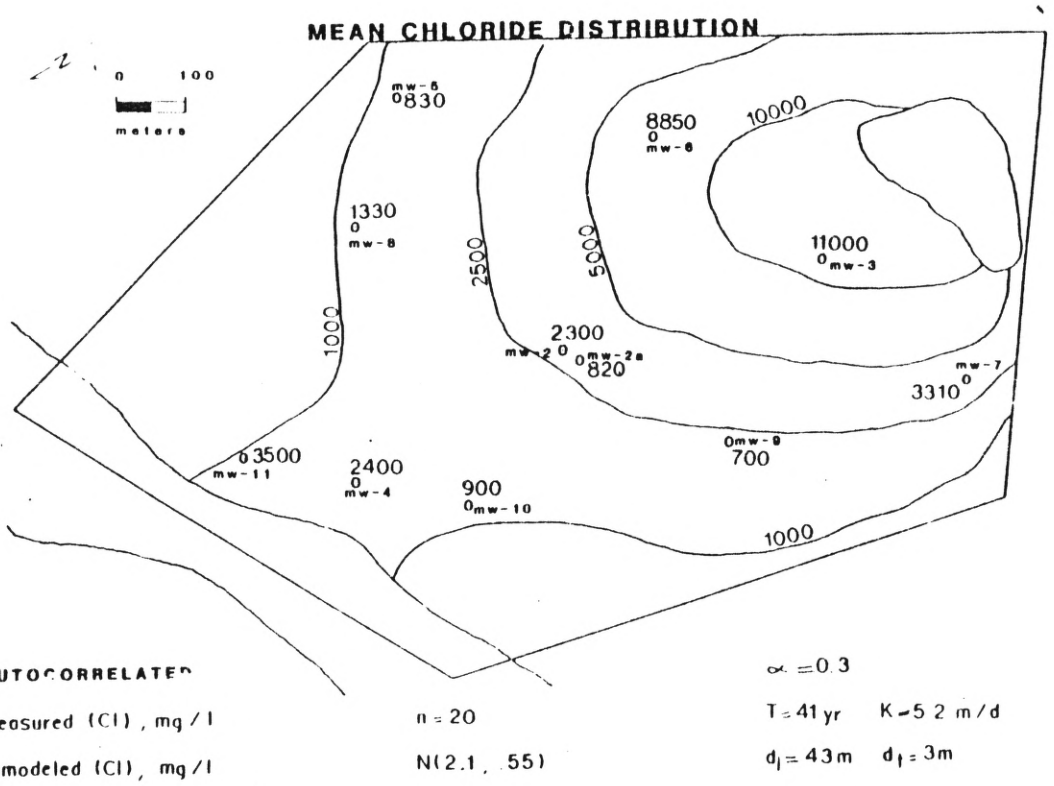

Figure 32. Mean chloride distribution produced by the autocorrelated log-normal hydraulic conductivity distribution, alpha=0.3.

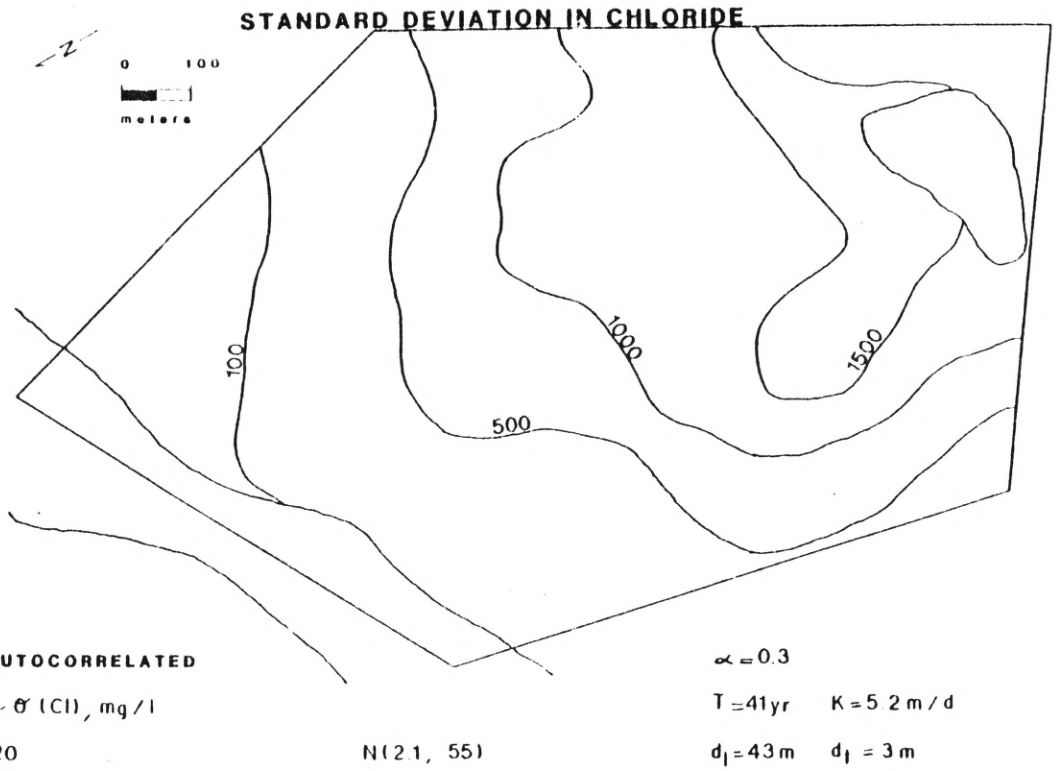

Figure 33. Standard deviation in chloride produced by the autocorrelated log-normal hydraulic conductivity distribution, alpha=0.3.

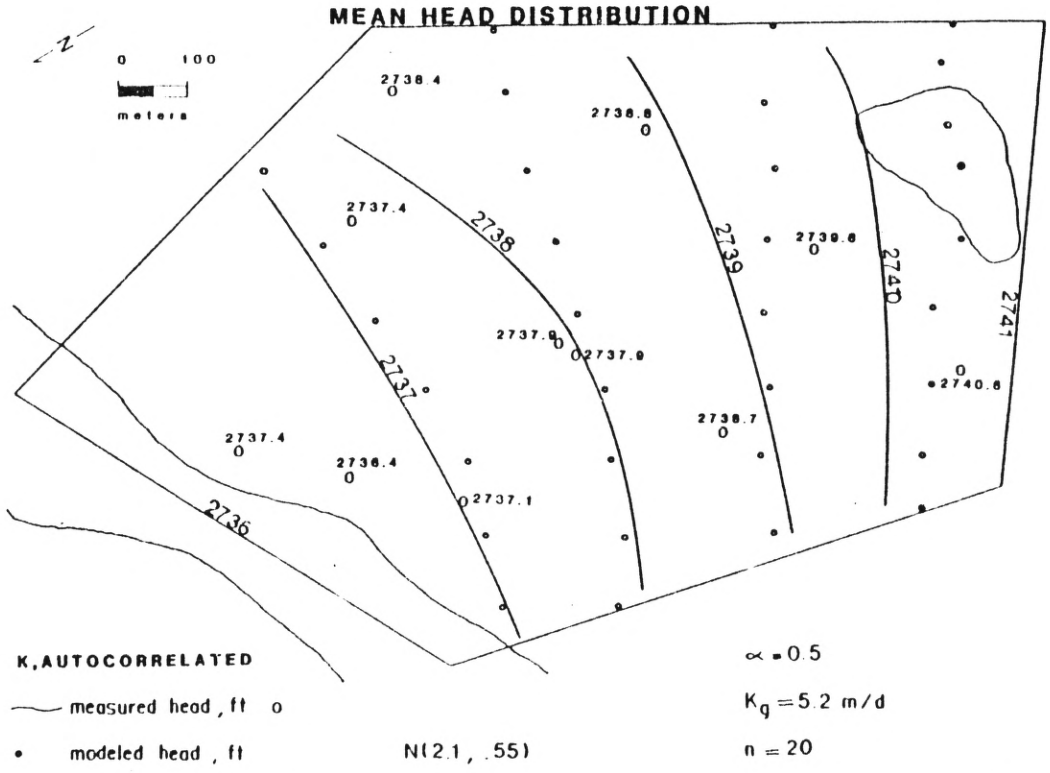

Figure 34. Mean hydraulic head distribution produced by the autocorrelated log-normal hydraulic conductivity distribution, alpha=0.5.

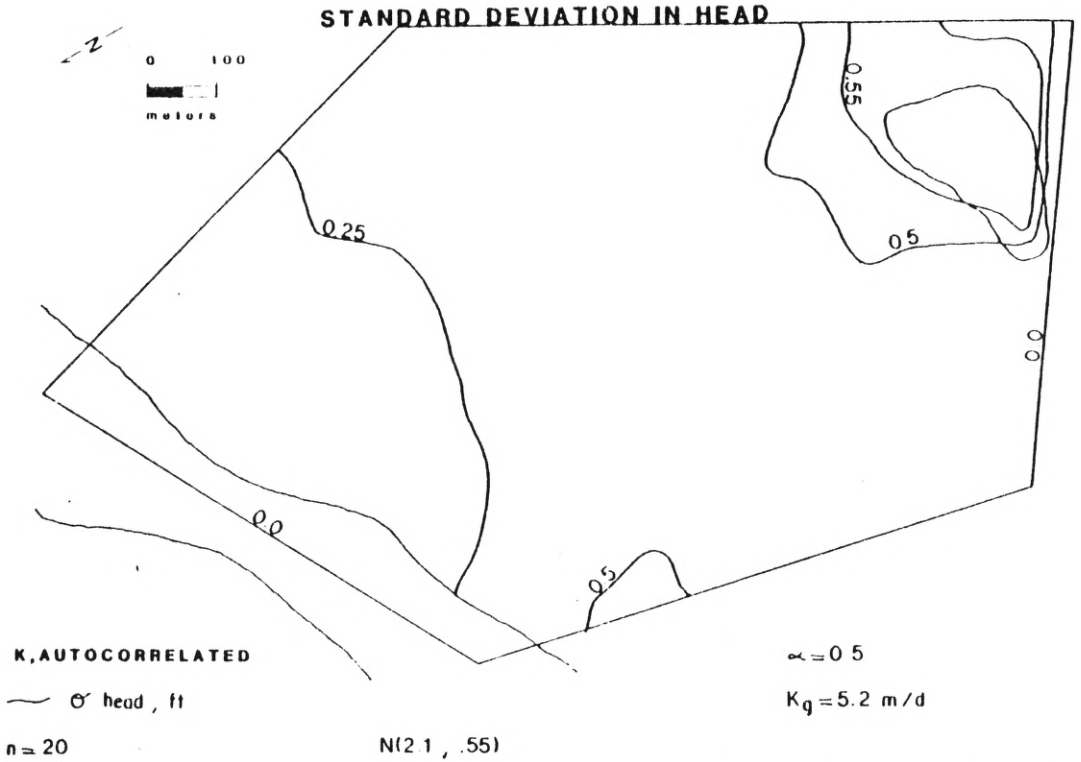

Figure 35. Standard deviation in hydraulic head produced by the autocorrelated log-normal hydraulic conductivity distribution, alpha=0.5.

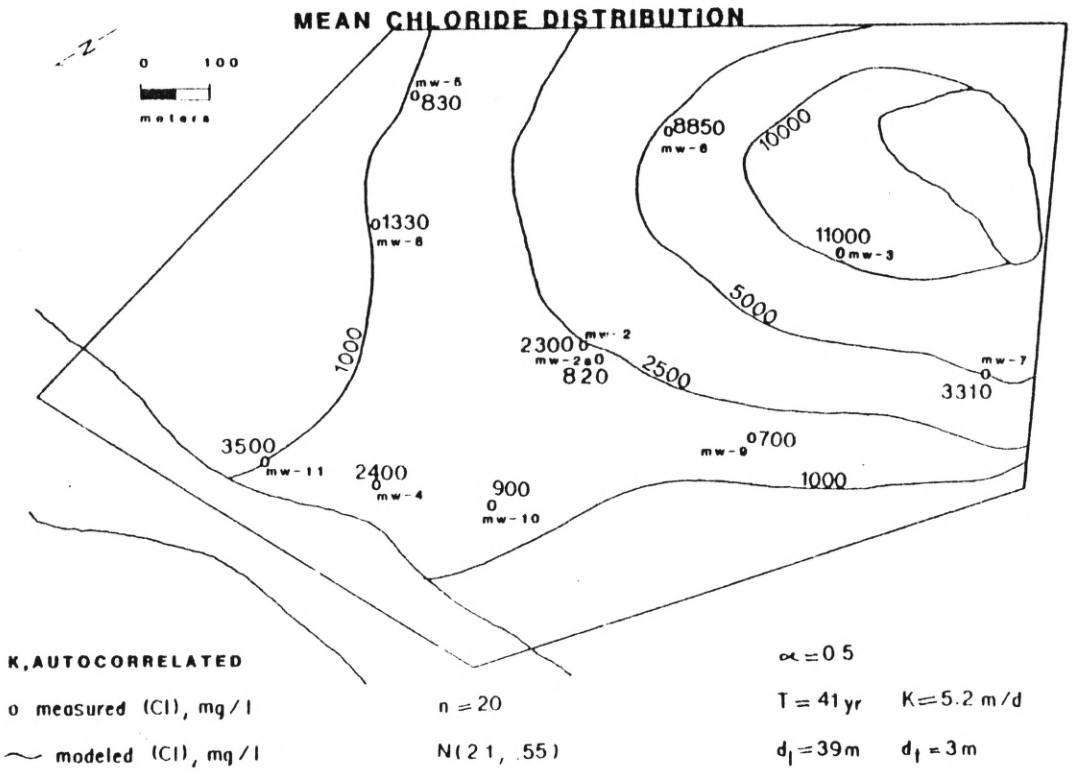

Figure 36. Mean chloride distribution produced by the autocorrelated log-normal hydraulic conductivity distribution, alpha=0.5.

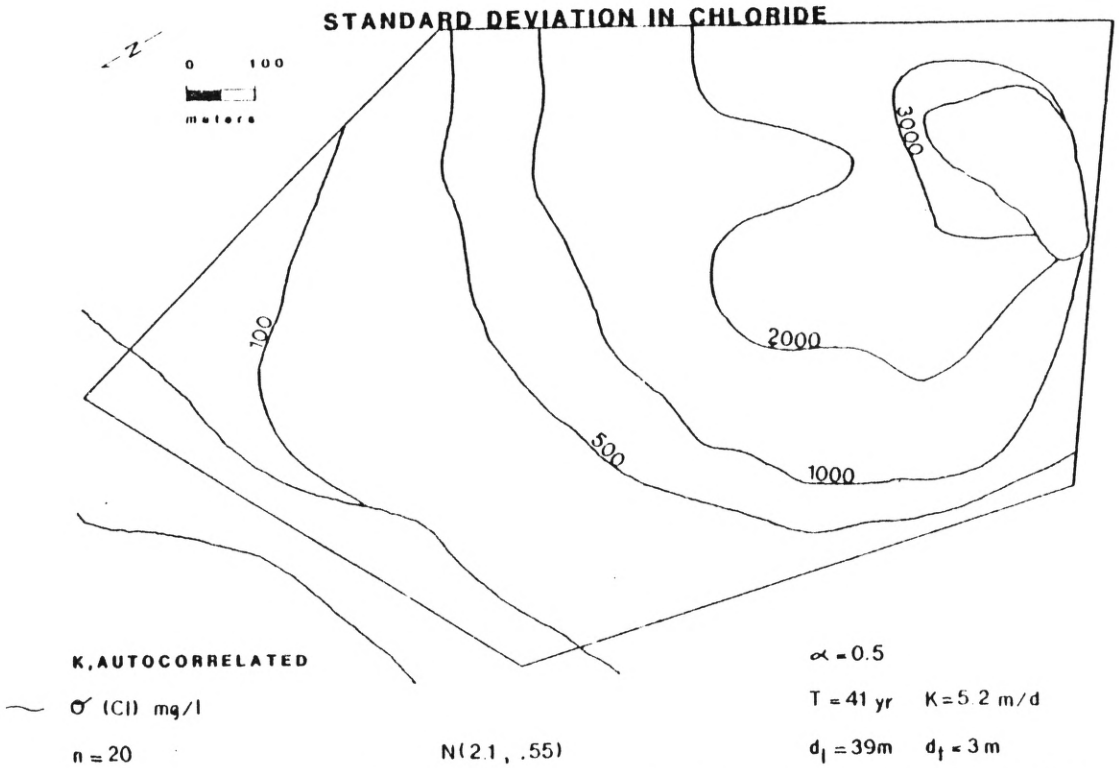

Figure 37. Standard deviation in chloride produced by the autocorrelated log-normal hydraulic conductivity distribution, alpha=0.5.

with alph equal to 0.0.

The degree of uncertainty in heads was greater for alpha equal to 0.5 than it was for alpha equal to 0.3. The greatest uncertainty in hydraulic heads (0.5 feet) was only 10% of the total head drop across the flow system for alpha equal to 0.3. It was 15% of the total head drop in the system where alpha was equal to 0.5. The percentage of the total head drop across the flow system was the same for alpha equal to 0.3 and 0.7. The percentage was the greatest for alpha equal to 0.5. However, the area encompassed by high uncertainty in hydraulic head increased systematically as the degree of autocorrelation in conductivities increased (Figs. 21, 26, 31, and 35). The explanation for this was given in the discussion of the model results obtained when alpha was equal to 0.7.

The smallest dispersivities, d_l=30 meters and d_t=3 meters, were used with alpha equal to 0.7. The largest dispersivities, d_l=46 meters and d_t= 9 meters, were obtained with alpha equal to 0.0. In general, as the degree of autocorrelation in hydraulic conductivities increased, the dependence on dispersivities to produce large-scale mixing decreased. In other words, large-scale mixing was created by macroscopic variations in hydraulic conductivity as those conductivities became spatially related to each other.

The standard deviation in dissolved chloride increased as the degree of autocorrelation in conductivities increased (Figs. 24, 29, 33, and 37). The uncertainty in dissolved chloride ranged from as little as 100 mg/l for alpha equal to 0.0 to as much as 4000 mg/l for alpha equal

to 0.7. This represents 14% of the smallest measured chloride concentration (700 mg/l in MW-9) to over 500% of the smallest measured chloride concentration.

The summation of velocities in the x- and y-directions is a measure of the degree of confinement of groundwater flow to specific zones in the system. Table II lists the summations of velocities for the hydraulic conductivity distributions used in this study. As the degree of autocorrelation of conductivities increased, the summations of velocities in the x- and y-directions decreased. This could not reflect a decrease in all velocities in the system because, as autocorrelation increased, smaller dispersivities were required in order to reproduce the observed chloride distribution. Equation 19 also illustrates this fact. The total displacement of chloride was approximately the same for all of the autocorrelated models even though the dispersivities were different. The only way this could happen is if the velocities increased as dispersivities decreased. It must signify increased isolation of groundwater flow in zones of high conductivity as autocorrelation in conductivities increased. The smallest sums correspond to the autocorrelated hydraulic conductivity distribution requiring the smallest dispersivities to obtain an acceptable match between observed and modeled chloride distributions.

VIII. CONCLUSIONS

Both theoretical and field-related conclusions could be drawn from the results of this study.

The amount of dissolved chloride dispersion in the system increased with increasing autocorrelation of the log-normal conductivity

SUM OF VELOCITIES IN X+Y DIRECTIONS

$\sum V_x$ (m/d)	$\sum V_y$ (m/d)	α
7.64	3.13	K, homogeneous
7.44	4.85	0.0
1.90	1.24	0.3
1.82	1.04	0.5
1.71	1.04	0.7

Table II. The summations of velocities in the x- and y-directions for the five hydraulic conductivity distributions used in this study.

distribution. The increased spreading was created by groundwater flowing along interconnected high conductivity zones.

Uncertainty in the mean head and dissolved chloride distributions increased with increasing autocorrelation of the conductivity distribution. The greatest uncertainty was observed in zones of high hydraulic gradient, such as beneath the pond and along the western no-flow boundary, and in regions furthest removed from the constant head boundaries. The amount of uncertainty in the mean hydraulic head and dissolved chloride distributions would be decreased (possibly by an order of magnitude) in going from a one-, to a two-, to a three-dimensional flow model. Increased dispersion of dissolved chloride would be produced (for the same value of alpha) in going from a one-, to a two-, to a three-dimensional flow model.

The summation of velocities in the x- and y-directions indicates that groundwater flow becomes increasingly confined to high conductivity zones as autocorrelation of the conductivity distribution increases. This is supported by the smaller dispersivities required with larger values of alpha (Table II).

No direct relationship was observed between the quality of the match between observed and calculated heads as autocorrelation of the conductivities increased.

Field conclusions are 1) large-scale mixing of dissolved chloride was produced by autocorrelated log-normal hydraulic conductivity distributions, 2) there was a reduction in the amount of longitudinal spreading of the chloride with a random log-normal conductivity distribution,

3) the longitudinal dispersivity (46 meters) used in the deterministic model was reduced by 16 meters for alpha equal to 0.7. A summary of the dispersivity versus alpha trend can be found in Table III. Fourth, the dissolved chloride plume moved approximately 10 meters/year, however, because of large-scale mixing of the dissolved chloride, the 1,000 mg/l isochore reached the Canadian River. Fifth, the dissolved chloride measured at certain wells suggest that either a three-dimensional or profile-oriented transport model would be required to simulate some of the observed transport phenomena. Finally, the best match between observed and calculated dissolved chloride distributions was obtained when using an autocorrelated log-normal hydraulic conductivity distribution with alpha equal to 0.7.

DISPERSIVITIES vs. α

d_1 (m)	d_4 (m)	α
46	9	K, homogeneous
46 +	3	0.0
43	3	0.3
39	3	0.5
30	3	0.7

Table III. Summary of the dispersivity versus alpha for the five hydraulic conductivity distributions used in this study.

APPENDIX A

Dimensions (M, mass; L, distance; T, time; C, concentration) are given in parentheses.

v	groundwater velocity	(L/T)
K	hydraulic conductivity	(L/T)
ϕ	porosity	
h	hydraulic head	(L)
R	source/sink term	(1/T)
S_s	specific storage	(1/L)
F	mass flux	(M/L**2T)
D	coefficient of molecular diffusion	(L**2/T)
C	concentration	(M/L**3)
D_{ij}	coefficient of mechanical dispersion	(L**2/T)
d_t	transverse dispersivity	(L)
d_l	longitudinal dispersivity	(L)
v_i	velocity in the x-direction	(L/T)
v_j	velocity in the y-direction	(L/T)
v_{ij}	resultant velocity	(L/T)
σ	standard deviation	
u	arithmetic mean	
D_h	coefficient of hydrodynamic dispersion	(L**2/T)
W	source/sink term	(M/L**3T)
T	transmissivity	(L**2/T)
Y_{ij}	random variable satisfying the autocorrelation relation	
ϵ_{ij}	normal, random distribution of numbers with mean=0 and σ =1	
$[W]$	matrix of scaled weights	
r	total number of blocks surrounding block k	
η	multiplication factor	

APPENDIX B

```
      PROGRAM MWALK (INPUT, OUTPUT, TAPE5=INPUT, TAPE6=OUTPUT)
C
C*** ILLINOIS STATE WATER SURVEY
C*** MASS TRANSPORT CODE WITH
C*** OR WITHOUT DISPERSION AND RETARDATION.
C
C*** THE TRANSPORT CODE IS THE FOLLOWING:
C*** DISPERSION--RANDOM WALK
C*** CONVECTION--PARTICLE-IN-A-CELL
C*** THE FOLLOWING COMMENT CARDS DOCUMENT CHANGES IN BULL. 65,
C*** PRICKETT AND OTHERS , MADE BY PBM.  THE REST OF THE CODE
C*** IS DESCRIBED IN BULL. 65.
C
      DIMENSION IP(100), JP(100), P(100,12)
      DIMENSION VOL(44,28)
      COMMON/RETARD/ RD1,KD,RHO
      REAL KD
      COMMON/EXTRA/ PERM(44,34,2), T(44,34,2), SF1(44,34), SF2(44,34)
      COMMON/EXTRA3/ ITER,NSTEPS,DL(44,34), ISTEP
      COMMON/POR/ APOR, EPOR, CONSOR(44,34)
      COMMON/VEL/ NC, NR, ANC, ANR, V(44,34,2)
      COMMON/TRACE/ NP, MAXP, PM, DISPL, DISPT, X(5001), Y(5001), MARK
     1(44,34), TMAP
      COMMON/EXTRA2/ CH(44,34), HO(44,34), G(44), B(44), R(44,34), TIME,
     1ERROR, E
      COMMON/AQUI/ H(44,34), RH(44,34), DELTA, Q(44,34), SOR(44,34)
      COMMON/VAR/ DELX(50), DELY(50)
      COMMON/AQUI2/ RD(44,34), BOT(44,34)
      COMMON/POL/ X1, DX, Y1, DY, DELP
      INTEGER OUT
      CALL SECOND(T)
      CALL RANSET(T)
C*** READ AND WRITE INPUT VALUES
      READ(5,10) NSTEPS, DELTA, ERROR, NPITS
     1,NC,NR,TT,S1,HH,QQ,RR,RRH,RRD,S2,CCH,PP,BOTT
10    FORMAT(I6,2F6.0,I6/2I6,11F6.0)
      WRITE(6,20)
20    FORMAT(" ","VALUES ON PARAMETER CARD")
      WRITE(6,30)
30    FORMAT(" ","NSTEPS",4X,"DELTA",4X,"ERROR",4X,"NPITS")
      WRITE(6,40)NSTEPS,DELTA,ERROR,NPITS
40    FORMAT(1X,I7,2X,E7.2,2X,E7.2,1X,I7)
      WRITE(6,50)
50    FORMAT("0","VALUES ON DEFAULT VALUE CARDS")
      WRITE(6,60)
60    FORMAT(" ", 1X,"NC",1X,"NR",9X,"TT",9X,"S1",9X,"S2",9X,"HH",9X,"QQ",
     19X,"RR",4X,"RRH",4X,"PP",3X,"BOTT",4X,"RRD",4X,"CCH")
      WRITE(6,70)NC,NR,TT,S1,S2,HH,QQ,RR,RRH,PP,BOTT,RRD,CCH
70    FORMAT(" ",2I3,F11.3,5F11.5,2F7.0,3F7.2)
      READ(5,80)NPUMP,NSP,NRT
80    FORMAT(3I6)
```

```
      WRITE(6,90)
90    FORMAT("0",1X,"PUMP PARAMETER VALUES")
      WRITE(6,100)
100   FORMAT(" ",2X,"NPUMP",3X,"NSP",3X,"NRT")
      WRITE(6,110)NPUMP,NST,NRT
110   FORMAT(" ",1X,3I6)
      DO 130 I=1,NPUMP
      READ(5,120)IP(I),JP(I),(P(I,K),K=1,NRT)
120   FORMAT(2I3,12F6.0)
130   CONTINUE
      WRITE(6,140)
140   FORMAT("0",1X,"PUMPING SCHEDULES")
      WRITE(6,150)
150   FORMAT(" ",1X,"IP",1X,"JP",8X,"P1",8X,"P2",8X,"P3",8x,"P4",8X,"P5",
     18X,"P6",8X,"P7",8X,"P8",8X,"P9",7X,"P10",7X,"P11",7X,"P12")
      DO 170 I=1,NPUMP
      WRITE(6,160)IP(I),JP(I),(P(I,M),M=1,NRT)
160   FORMAT(" ",1X,2I3,2X,12F10.3)
170   CONTINUE
      READ(5,180)(DELX(I),I=1,NC)
180   FORMAT(10F8.0)
      READ(5,180)(DELY(J),J=1,NR)
      WRITE(6,190)
190   FORMAT("0",5X,"VALUES OF ROW J AND DELY")
      DO 210 J=1,NR
      WRITE(6,200)J,DELY(J)
200   FORMAT(" ",15X,I5,1X,F8.0)
210   CONTINUE
      WRITE(6,220)
220   FORMAT("0",1X,"VALUES OF COLUMN I AND DELX")
      DO 240 I=1,NC
      WRITE(6,230)I,DELX(I)
230   FORMAT(" ",14X,I5,1X,F8.0)
240   CONTINUE
      DO 260 I=1,NC
      DO 250 J=1,NR
      T(I,J,1)=TT
      T(I,J,2)=TT
      PERM(I,J,1)=PP
      PERM(I,J,2)=PP
      SF1(I,J)=S1
      SF2(I,J)=S2
      H(I,J)=HH
      HO(I,J)=HH
      R(I,J)=RR
      RH(I,J)=RRH
      RD(I,J)=RRD
      CH(I,J)=CCH
      BOT(I,J)=BOTT
      DL(I,J)=0.0
```

```
      Q(I,J)=QQ
250   CONTINUE
260   CONTINUE
      READ(5,270)X1,DX,Y1,DY,DELP
270   FORMAT(5F10.0)
      WRITE(6,280)
280   FORMAT("0",1X,"INITIAL LOCATION OF PARTICLES")
      WRITE(6,290)
290   FORMAT(" ",1X,"AND TIME INCREMENT DELP")
      WRITE(6,300)
300   FORMAT(" ",8X,"X1",8X,"DX",8X,"Y1",8X,"DY",6X,"DELP")
      WRITE(6,305)X1,DX,Y1,DY,DELP
305   FORMAT(" ",5F10.0)
      READ(5,310)PL,MAXP,PM,DISPL,DISPT,EPOR,APOR,RD1,KD,RHO
310   FORMAT(F7.1,I7,8F7.1)
      CALL RDSOLV(EPOR,RHO,KD,RD1)
      WRITE(6,320)
320   FORMAT("0",1X,"VALUES OF POLLUTION PARAMETERS")
      WRITE(6,330)
330   FORMAT(" ",8X,"PL",6X,"MAXP",8X,"PM",6X,"DISPL",3X,"DISPT",7X,
     1"EPOR",6X,"APOR",6X,"RD",7X,"KD",6X,"RHO")
      WRITE(6,340)PL,MAXP,PM,DISPL,DISPT,EPOR,APOR,RD1,KD,RHO
340   FORMAT(" ",1F10.0,I10,3F10.3,5F10.3)
      CALL INIT
      WRITE(6,343)
343   FORMAT("0",1X,"LOCATIONS OF SINKS AND IDENTIFIER")
      WRITE(6,345)
345   FORMAT(" ",2X,"I",2X,"J",1X,"MARK")
350   READ(5,360)I,J,MARK
360   FORMAT(3I3)
      IF(I.EQ.0.AND.J.EQ.0) GO TO 390
      MARK(I,J)=MARK
      WRITE(6,361)I,J,MARK(I,J)
361   FORMAT(" ",3I3)
      GO TO 350
390   CONTINUE
      WRITE(6,400)
400   FORMAT("0",1X,"LOCATIONS OF SOURCES AND THEIR CONCENTRATIONS")
410   READ(5,420)I,J,CONSOR(I,J)
420   FORMAT(2I3,1F14.4)
      IF(I.EQ.0.AND.J.EQ.0) GO TO 430
      WRITE(6,421)I,J,CONSOR(I,J)
421   FORMAT(" ",2I3,1F14.4)
      GO TO 410
430   CONTINUE
      DO 435 I=1,NC
435   READ(5,436)(PERM(I,J,1),J=1,NR)
436   FORMAT(10F7.0)
      DO 437 I=1,NC
      DO 437 J=1,NR
      PERM(I,J,2)=PERM(I,J,1)
```

```
      T(I,J,1)=PERM(I,J,1)*94.
      T(I,J,2)=PERM(I,J,2)*94.
437   CONTINUE
C*** SET CONDUCTIVITIES TO 0.0 FOR NODES OUTSIDE BOUNDARIES
      PERM(1,1,1)=0.0
      PERM(1,1,2)=0.0
      PERM(1,2,1)=0.0
      PERM(1,2,2)=0.0
      PERM(1,3,1)=0.0
      PERM(1,3,2)=0.0
      PERM(1,4,1)=0.0
      PERM(1,4,2)=0.0
      PERM(1,5,1)=0.0
      PERM(1,5,2)=0.0
      PERM(1,7,1)=0.0
      PERM(1,7,2)=0.0
      PERM(1,8,1)=0.0
      PERM(1,8,2)=0.0
      PERM(1,9,1)=0.0
      PERM(1,9,2)=0.0
      PERM(1,10,1)=0.0
      PERM(1,10,2)=0.0
      PERM(2,1,1)=0.0
      PERM(2,1,2)=0.0
      PERM(2,2,1)=0.0
      PERM(2,2,2)=0.0
      PERM(2,3,1)=0.0
      PERM(2,3,2)=0.0
      PERM(2,4,1)=0.0
      PERM(2,4,2)=0.0
      PERM(2,8,1)=0.0
      PERM(2,8,2)=0.0
      PERM(2,9,1)=0.0
      PERM(2,9,2)=0.0
      PERM(2,10,1)=0.0
      PERM(2,10,2)=0.0
      PERM(3,1,1)=0.0
      PERM(3,1,2)=0.0
      PERM(3,2,1)=0.0
      PERM(3,2,2)=0.0
      PERM(3,3,1)=0.0
      PERM(3,3,2)=0.0
      PERM(3,8,1)=0.0
      PERM(3,8,2)=0.0
      PERM(3,9,1)=0.0
      PERM(3,9,2)=0.0
      PERM(3,10,1)=0.0
      PERM(3,10,2)=0.0
      PERM(4,1,1)=0.0
      PERM(4,1,2)=0.0
      PERM(4,2,1)=0.0
```

```
PERM(4,2,2)=0.0
PERM(4,3,1)=0.0
PERM(4,3,2)=0.0
PERM(4,8,1)=0.0
PERM(4,8,2)=0.0
PERM(4,9,1)=0.0
PERM(4,9,2)=0.0
PERM(4,10,1)=0.0
PERM(4,10,2)=0.0
PERM(5,1,1)=0.0
PERM(5,1,2)=0.0
PERM(5,2,1)=0.0
PERM(5,2,2)=0.0
PERM(5,9,1)=0.0
PERM(5,9,2)=0.0
PERM(5,10,1)=0.0
PERM(5,10,2)=0.0
PERM(6,1,1)=0.0
PERM(6,1,2)=0.0
PERM(6,9,1)=0.0
PERM(6,9,2)=0.0
PERM(6,10,1)=0.0
PERM(6,10,2)=0.0
PERM(7,10,1)=0.0
PERM(7,10,2)=0.0
PERM(8,10,1)=0.0
PERM(8,10,2)=0.0
PERM(11,10,1)=0.0
PERM(11,10,2)=0.0
PERM(12,10,1)=0.0
PERM(12,10,2)=0.0
PERM(13,10,1)=0.0
PERM(13,10,2)=0.0
PERM(14,10,1)=0.0
PERM(14,10,2)=0.0
PERM(15,9,1)=0.0
PERM(15,9,2)=0.0
PERM(15,10,1)=0.0
PERM(15,10,2)=0.0
PERM(16,9,1)=0.0
PERM(19,9,2)=0.0
PERM(16,10,1)=0.0
PERM(16,10,2)=0.0
PERM(17,9,1)=0.0
PERM(17,9,2)=0.0
PERM(17,10,1)=0.0
PERM(17,10,2)=0.0
PERM(18,9,1)=0.0
PERM(18,9,2)=0.0
PERM(18,10,1)=0.0
PERM(18,10,2)=0.0
```

```
      PERM(19,9,1)=0.0
      PERM(19,9,2)=0.0
      PERM(19,10,1)=0.0
      PERM(19,10,2)=0.0
      PERM(20,8,1)=0.0
      PERM(20,8,2)=0.0
      PERM(20,9,1)=0.0
      PERM(20,9,2)=0.0
      PERM(20,10,1)=0.0
      PERM(20,10,2)=0.0
C***  SET STORATIVITIES TO 0.0 AT CONSTANT HEAD NODES
      SF1(1,6)=1E-10
      SF1(2,7)=1E-10
      SF1(3,7)=1E-10
      SF1(4,7)=1E-10
      SF1(5,8)=1E-10
      SF1(6,8)=1E-10
      SF1(7,9)=1E-10
      SF1(8,9)=1E-10
      SF1(20,2)=1E-10
      SF1(20,3)=1E-10
      SF1(20,4)=1E-10
      SF1(20,5)=1E-10
      SF1(20,6)=1E-10
      SF1(20,7)=1E-10
C***  SET CONSTANT HEAD NODES
      H(1,6)=2736.
      H(2,7)=2736.
      H(3,7)=2736.
      H(4,7)=2736.
      H(5,8)=2736.
      H(6,8)=2736.
      H(7,9)=2736.
      H(8,9)=2736.
      H(20,2)=2741.
      H(20,3)=2741.
      H(20,4)=2741.
      H(20,5)=2741.
      H(20,6)=2741.
      H(20,7)=2741.
      DELY(20)=360.
      DELY(6)=360.
      DO 510 I=1,NC
      DO 500 J=1,NR
      V(I,J,1)=0.0
      V(I,J,2)=0.0
500   CONTINUE
510   CONTINUE
      TIME=0
      DELI=DELTA
      KC=1
```

```
      DO 630 ISTEP=1,NSTEPS
      IF(NPUMP.EQ.0) GO TO 535
      Z=(ISTEP-1.0)/NSP+1.0
      IF(Z-KC)540,520,540
520   CONTINUE
      DO 530 K=1,NPUMP
      I=IP(K)
      J=JP(K)
      Q(I,J)=P(K,KC)
530       CONTINUE
535   CONTINUE
      DELTA=DELI
      KC=KC+1
540   CONTINUE
      CALL CLEAR
C*** CALL SUBROUTINE TO SOLVE FLOW EQUATION
      CALL HSOLVE
      DO 580 I=1,NC
580   WRITE(6,570)(H(I,J),J=1,NR)
570   FORMAT(" ",F7.2,9F8.2)
      DO 610 I=1,NC
      DO 600 J=1,NR
      IF(J.NE.NR)V(I,J,1)=-PERM(I,J,1)*(H(I,J+1)-H(I,J))/(DELX(I)
     1*EPOR*7.48052)
      IF(I.NE.NC)V(I,J,2)=-PERM(I,J,2)*(H(I+1,J)-H(I,J))/(DELY(J)
     1*EPOR*7.48052)
600   CONTINUE
610   CONTINUE
C*** MOVE PARTICLES NPITS TIME STEPS
      DO 620 I=1,NPITS
      CALL CLEAR
      CALL ADVAN(DELP)
      CALL SOURCE
      CALL MAP
620   CONTINUE
      DELTA=DELTA
630   CONTINUE
C*** SUM VELOCITIES IN X- AND Y-DIRECTIONS
      OLDVX=0.0
      OLDVY=0.0
      DO 850 I=1,NC
      DO 850 J=1,NR
      IF(PERM(I,J,1).EQ.0.0) GO TO 850
      VX=V(I,J,2)+OLDVX
      VY=V(I,J,1)+OLDVY
      OLDVX=VX
      OLDVY=VY
850   CONTINUE
      VECTOR=SQRT(OLDVX**2+OLDVY**2)
      WRITE(6,860)
860   FORMAT(" ",////)
```

```
      WRITE(6,870)OLDVX,OLDVY,VECTOR
870   FORMAT(" ",3F20.4)
      STOP
      END
      SUBROUTINE ADD(XX,YY)
      COMMON/TRACE/ NP,MAXP,PM,DISPL,DISPT,X(5001),Y(5001),MARK(44,34),
     1TMAP
      NP=NP+1
      X(NP)=XX
      Y(NP)=YY
      IF(NP.LT.MAXP)RETURN
      K=RANF(0)*MAXP+1.0
      X(K)=X(NP)
      Y(K)=Y(NP)
      PM=PM*MAXP/(MAXP-1)
      NP=NP-1
      RETURN
      END
      SUBROUTINE ADVAN(DELP)
      COMMON/TRACE/ NP,NAXP,PM,DISPL,DISPT,X(5001),Y(5001),MARK(44,34)
     1TMAP
      TMAP=TMAP+DELP
      K=0
1     K=K+1
2     IF(K.GT.NP) RETURN
      IF(MOVE(X(K),Y(K),DELP).EQ.0) GO TO 1
      X(K)=X(NP)
      Y(K)=Y(NP)
      NP=NP-1
      GO TO 2
      END
      FUNCTION ANORM(K)
      ANORM=-6.0
      DO 10 I=1,12
      ANORM=ANORM+RANF(0)
10    CONTINUE
      RETURN
      END
      SUBROUTINE CLEAR
      COMMON/VEL/ NC,NR,ANC,ANR,V(44,34,2)
      COMMON/FORMS/ TABLE(50),NPART(44,34)
      DO 20 I=1,NC
      DO 10 J=1,NR
      NPART(I,J)=0
10    CONTINUE
20    CONTINUE
      DO 30 I=1,50
      TABLE(I)=0.0
30    CONTINUE
      RETURN
      END
```

```
      SUBROUTINE GENP(PL)
      COMMON/TRACE/ NP,MAXP,PM,DISPL,DISPT,
      COMMON/POL/ X1,DX,Y1,DY,DELP
      P=PL
1     IF(RANF(0).GT.P/PM) RETURN
      P=P-PM
      XX=X1+DX*RANF(0)
      YY=Y1+DY*RANF(0)
      DE=DELP*RANF(0)
      IF(MOVE(XX,YY,DE).EQ.0) CALL ADD(XX,YY)
      GO TO 1
      END
      SUBROUTINE HSOLVE
C*** ADI METHOD OF PRICKETT AND OTHERS REPLACED BY SOR METHOD AS
C*** DESCRIBED BY WANG AND ANDERSON (1982)
      COMMON/EXTRA3/ ITER,NSTEPS,DL(44,34),ISTEP
      COMMON/EXTRA2/ CH(44,34),HO(44,34),G(44),BB(44),R(44,34),TIME,
     1ERROR,E
      COMMON/EXTRA/ PERM(44,34,2),T(44,34,2),SF1(44,34),SF2(44,34)
      COMMON/AQUI/ H(44,34),RH(44,34),DELTA,Q(44,34)
      COMMON/AQUI2/ RD(44,34),BOT(44,34)
      COMMON/VEL/ NC,NR,ANC,ANR,V(44,34,2)
      A=272./360.
      B=360./272.
      OMEGA=1.8
      NUMIT=0
30    AMAX=0.
      NUMIT=NUMIT+1
      IF(NUMIT.GT.1000) GO TO 40
      DO 40 I=1,NC
      DO 40 J=1,NR
      OLDVAL=H(I,J)
      IF(PERM(I,J,1).EQ.0.) GO TO 40
      IF(SF1(I,J).GT.100.) GO TO 40
      IF(I.EQ.1) GO TO 31
      IF(I.EQ.NC) GO TO 32
      IF(J.EQ.1) GO TO 33
      IF(J.EQ.NR) GO TO 34
      IF(PERM(I-1,J,1).EQ.0..AND.PERM(I,J-1,1).EQ.0.) GO TO 70
      IF(PERM(I-1,J,1).EQ.0..AND.PERM(I,J+1,1).EQ.0.) GO TO 71
      IF(PERMI+1,J,1).EQ.0..AND.PERM(I,J-1,1).EQ.0.) GO TO 72
      IF(PERM(I+1,J,1).EQ.0..AND.PERM(I,J+1,1).EQ.0.) GO TO 73
      IF(PERM(I-1,J,1).EQ.0.) GO TO 35
      IF(PERM(I+1,J,1).EQ.0.) GO TO 36
      IF(PERM(I,J-1,1).EQ.0.) GO TO 37
      IF(PERM(I,J+1,1).EQ.0.) GO TO 38
      H(I,J)=(B*T(I-1,J,1)*H(I-1,J) + B*T(I,J,2)*H(I+1,J) + A*T(I,J,1)*
     1H(I,J+1) + A*T(I,J-1,1)*H(I,J-1) + Q(I,J))/(B*T(I-1,J,2) +
     2B*T(I,J,2) + A*T(I,J,1) + A*T(I,J-1,1))
      GO TO 99
```

```
31    IF(PERM(I,J-1,1).EQ.0.) GO TO 39
      IF(PERM(I,J+1,1).EQ.0.) GO TO 41
      H(I,J)=(2.*B*T(I,J,2)*H(I+1,J) + A*T(I,J,1)*H(I,J+1) + A*T(I,J-1,1)
     1*H(I,J-1) + Q(I,J))/(2.*B*T(I,J,2) + A*T(I,J,1) + A*T(I,J-1,1))
      GO TO 99
32    IF(I.EQ.44..AND.J.EQ.1) GO TO 42
      IF(PERM(I,J-1,1).EQ.0.) GO TO 42
      IF(PERM(I,J+1,1).EQ.0.) GO TO 43
      H(I,J)=(2.*B*T(I-1,J,1)*H(I-1,J) + A*T(I,J,1)*H(I,J+1) + A*T(I,J-1,
     11)*H(I,J-1) + Q(I,J))/(2.*B*T(I-1,J,1) + A*T(I,J,1) + A*T(I,J-1,1))
      GO TO 99
33    IF(PERM(I-1,J,1).EQ.0.) GO TO 44
      IF(PERM(I+1,J,1).EQ.0.) GO TO 45
      H(I,J)=(B*T(I,J,2)*H(I+1,J) + B*T(I-1,J,1)*H(I-1,J) + 2.*A*T(I,J,1)
     1*H(I,J+1) + Q(I,J))/(B*T(I,J,2) + B*T(I-1,J,1) + 2.*A*T(I,J,1))
      GO TO 99
34    IF(PERM(I-1,J,1).EQ.0.) GO TO 46
      IF(PERM(I+1,J,1).EQ.0.) GO TO 47
      H(I,J)=(B*T(I,J,2)*H(I+1,J) + B*T(I-1,J,1)*H(I-1,J) + 2.*A*T(
     1I,J-1,1)*H(I,J-1) + Q(I,J))/(B*T(I,J,2) + B*T(I-1,J,2) + 2.*A*
     2T(I,J-1,1))
      GO TO 99
35    H(I,J)=(2.*B*T(I,J,2)*H(I=1,J) + A*T(I,J,1)*H(I,J+1) + A*T(I,J-1,1)
     1*H(I,J-1) + Q(I,J))/(2.*B*T(I,J,2) + A*T(I,J,1) + A*T(I,J-1,1))
      GO TO 99
36    H(I,J)=(2.*B*T(I-1,J,1)*H(I-1,J) + A*T(I,J,1)*H(I,J+1) + A*T(
     1I,J-1,1)*H(I,J-1) + Q(I,J))/(2.*B*T(I-1,J,1) + A*T(I,J,1) + A*T
     2(I,J-1,1))
      GO TO 99
37    H(I,J)=(B*T(I,J,2)*H(I+1,J) + B*T(I-1,J,1)*H(I-1,J) + 2.*A*T(I,J,1)
     1*H(I,J+1) + Q(I,J))/(B*T(I,J,2) + B*T(I-1,J,1) + 2.*A*T(I,J,1))
      GO TO 99
38    H(I,J)=(B*T(I,J,2)*H(I+1,J) + B*T(I-1,J,1)*H(I-1,J) + 2.*A*T(
     1I,J-1,1)*H(I,J-1) + Q(I,J))/(B*T(I,J,2) + B*T(I-1,J,2) + 2.*A*T(
     2I,J-1,1))
      GO TO 99
39    H(I,J)=(2.*B*T(I,J,2)*H(I+1,J) + 2.*A*T(I,J,1)*H(I,J+1) + Q(I,J))
     1/(2.*B*T(I,J,2) +2.*A*T(I,J,1))
      GO TO 99
41    H(I,J)=(2.*B*T(I,J,2)*H(I+1,J) + 2.*A*T(I,J-1,1)*H(I,J-1) + Q(I,J))
     1/(2.*B*T(I,J,2) + 2.*A*T(I,J-1,1))
      GO TO 99
42    H(I,J)=(2.*B*T(I-1,J,2)*H(I-1,J) + 2.*A*T(I,J,1)*H(I,J+1) + Q(I,J))
     1/(2.*B*T(I-1,J,2) +2.*A*T(I,J,1))
      GO TO 99
43    H(I,J)=(2.*B*T(I-1,J,2)*H(I-1,J) + 2.*A*T(I,J-1,1)*H(I,J-1) + Q(I,J
     1))/(2.*B*T(I-1,J,2) + 2.*A*T(I,J-1,1))
      GO TO 99
44    H(I,J)=(2.*B*T(I,J,2)*H(I+1,J) + 2.*A*T(I,J,1)*H(I,J+1) + Q(I,J))
     1/(2.*B*T(I,J,2) + 2.*A*T(I,J,1))
      GO TO 99
```

```
      H(I,J)=(2.*B*T(I-1,J,2)*H(I-1,J) + 2.*A*T(I,J,1)*H(I,J+1) + Q(I,J))
     1/(2.*B*T(I-1,J,2) + 2.*A*T(I,J,1))
      GO TO 99
46    H(I,J)=(2.*B*T(I,J,2)*H(I+1,J) + 2.*A*T*I,J-1,1)*H(I,J-1) + Q(I,J))
     1/(2.*B*T(I,J,2) + 2.*A*T(I,J-1,1))
      GO TO 99
47    H(I,J)=(2.*B*T(I-1,J,2)*H*I-1,J) + 2.*A*T(I,J-1,1)*H(I,J-1) + Q(I,J
     1))/(2.*B*T(I-1,J,2) +2.*A*T(I,J-1,1))
      GO TO 99
70    H(I,J)=(2.*B*T(I,J,2)*H(I+1,J) + 2.*A*T(I,J,1)*H(I,J+1) + Q(I,J))
     1/(2.*B*T(I,J,2) + 2.*A*T(I,J,1))
      GO TO 99
71    H(I,J)=(2.*B*T(I,J,2)*H(I+1,J) + 2.*A*T(I,J-1,1)*H(I,J-1) + Q(I,J))
     1/(2.*B*T(I,J,2) + 2.*A*T(I,J-1,1))
      GO TO 99
72    H(I,J)=(2.*B*T(I-1,J,2)*H(I-1,J) + 2.*A*T(I,J,1)*H(I,J+1) + Q(I,J))
     1/(2.*B*T(I-1,J,2) +2.*A*T(I,J,1))
      GO TO 99
73    H(I,J)=(2.*B*T(I-1,J,2)*H(I-1,J) + 2.*A*T(I,J-1,1)*H(I,J-1) + Q(I,J
     1))/(2.*B*T(I-1,J,2) + 2.*A*T(I,J-1,1))
99    H(I,J) =(OMEGA*H(I,J) + (1.-OMEGA)*OLDVAL
      ERR=ABS(H(I,J)-OLDVAL)
      IF(ERR.GT.AMAX)AMAX=ERR
40    CONTINUE
      IF(AMAX.GT.0.001) GO TO 30
      WRITE(6,50) NUMIT
50    FORMAT(///1X,I5)
      RETURN
      END
      SUBROUTINE INIT
      COMMON/TRACE/ NP,MAXP,PM,DISPL,DISPT,X(5001),Y(5001),MARK(44,34)
     1TMAP
      COMMON/AQUI/ H(44,34),RH(44,34),DELTA,Q(44,34),SOR(44,34)
      COMMON/EXTRA2/ CH(44,34),HO(44,34),G(44),B(44),R(44,34),TIME,
     1ERROR,E
      COMMON/VEL/ NC,NR,ANC,ANR,V(44,34,2)
      COMMON/POR/ APOR,EPOR,CONSOR(44,34)
      TMAP=0.
      NP=0
      ANC=NC+0.5
      ANR=NR+0.5
      DO 20 I=1,NC
      DO 10 J=1,NR
      SOR(I,J)=0.0
      CONSOR(I,J)=0.0
      MARK(I,J)=0
10    CONTINUE
20    CONTINUE
      RETURN
      END
      SUBROUTINE MAP
```

```
      REAL MOVAV(44,34)
      COMMON/TRACE/ NP,MAXP,PM,DISPL,DISPT,X(5001),Y(5001),MARK(44,34)
     1TMAP
      COMMON/FORMS/ TABLE(50),NPART(44,34)
      COMMON/VEL/ NC,NR,ANC,ANR,DELP
      WRITE(6,10)
10    FORMAT("0",1X,"MAP SHOWING NUMBER OF PARTICLES RESIDING IN THE
     1MODEL GRIDS")
      WRITE(6,20)PM,NP,TMAP
20    FORMAT("0","PARTICLE MASS= "E15.4/" ","NUMBER OF PARTICLES IN
     1SYSTEM= "I5/" ","TIME= ",F8.2,"DAYS")
      D) 614 I=1,NC
      DO 614 J=1,NR
      MOVAV(I,J)=0.
614   CONTINUE
C***  CALCULATE MOVING AVERAGES OF NUMBER OF PARTICLES?NODE
      DO 615 I=1,NC
      DO 615 J=1,NR
      IF(I.EQ.1.AND.J.EQ.1) GO TO 800
      IF(I.EQ.NC.AND.J.EQ.1) GO TO 801
      IF(I.EQ.1.AND.J.EQ.NR) GO TO 802
      IF(I.EQ.NC.AND.J.EQ.NR) GO TO 803
      IF(J.EQ.1) GO TO 804
      IF(J.EQ.NR) GO TO 805
      IF(I.EQ.1) GO TO 806
      IF(I.EQ.NC) GO TO 807
      GO TO 808
800   MOVAV(I,J)=(NPART(I,J)+NPART(I+1,J)+NPART(I,J+1)+NPART(I+1,J+1))/4.
      GO TO 615
801   MOVAV(I,J)=(NPART(I,J)+NPART(I-1,J)+NPART(I,J+1)+NPART(I-1,J+1))/4.
      GO TO 615
802   MOVAV(I,J)=(NPART(I,J)+NPART(I,J-1)+NPART(I+1,J)+NPART(I+1,J-1))/4.
      GO TO 615
803   MOVAV(I,J)=(NPART(I,J)+NPART(I,J-1)+NPART(I-1,J)+NPART(I-1,J-1))/4.
      GO TO 615
804   MOVAV(I,J)=(NPART(I,J)+NPART(I+1,J)+NPART(I-1,J)+NPART(I,J+1)+
     1NPART(I-1,J+1)+NPART(I+1,J+1))/6.
      GO TO 615
805   MOVAV(I,J)=(NPART(I,J)+NPART(I+1,J)+NPART(I-1,J)+NPART(I-1,J-1)+
     1NPART(I,J-1)+NPART(I+1,J-1))/6.
      GO TO 615
806   MOVAV(I,J)=(NPART(I,J)+NPART(I,J-1)+NPART(I,J+1)+NPART(I+1,J)+
     1NPART(I+1,J-1)+NPART(I+1,J+1))/6.
      GO TO 615
807   MOVAV(I,J)=(NPART(I,J)+NPART(I,J-1)+NPART(I,J+1)+NPART(I-1,J-1)+
     1NPART(I-1,J)+NPART(I-1,J+1))/6.
      GO TO 615
808   MOVAV(I,J)=(NPART(I,J)+NPART(I+1,J)+NPART(I,J+1)+NPART(I-1,J)+
     1NPART(I,J-1)+NPART(I-1,J-1)+NPART(I+1,J-1)+NPART(I-1,J+1)+NPART
     2(I+1,J+1))/9.
615   CONTINUE
```

```
      DO 40 I=1,NC
40    WRITE(6,30)(MOVAV(I,J),J=1,NR)
30    FORMAT(" ",F7.2,9F8.2)
      RETURN
      END
      FUNCTION MOVE(XX,YY,DEL)
      COMMON/VAR/ DELX(50),DELY(50)
      COMMON/TRACE/ NP,MAXP,PM,DISPL,DISPT,X(5001),Y(5001),MARK(44,34)
     1TMAP
      COMMON/FORMS/ TABLE(50),NPART(44,34)
      COMMON/VEL/ NC,NR,ANC,ANR,V(44,34,2)
      COMMON/RETARD/ RD1,KD,RHO
      REAL KD
      D=DEL
      DMIX=1/(2*DISPL)
1     IF(D.LE.0.0) GO TO 2
      CALL VELO(XX,YY,VX,VY)
      IXX=XX
      IYY=YY
      T=AMIN1(D,.2*ABS(DELX(IXX)/VX),.2*ABS(DELY(IYY)/VY))
      IF(VX.EQ.0.) T=AMIN1(D,.2*ABS(DELY(IYY)/VY))
      IF(VY.EQ.0.) T=AMIN1(D,.2*ABS(DELX(IXX)/VX))
      IF(VX.EQ.0..AND.VY.EQ.0.) T=D
      D=D-T
      DX=VX*T
      DY=VY*T
      SIGNX=1.0
      SIGNY=1.0
      IF(DX.LT.0.0) SIGNX=-1.0
      IF(DY.LT.0.0) SIGNY=-1.0
      IF(DX.EQ.0.0) DX=1E-30
      IF(DY.EQ.0.0) DY=1E-30
      PHI=ATAN(DY/DX)
      DD=SQRT(DX**2 + DY**2)/RD1
      IF(DD.EQ.0.0) DD=1E-30
      RL=(SQRT(2*DISPL*DD)/DD)*ANORM(0)
      RT=(SQRT(2*DISPT*DD)/DD)*ANORM(0)
      IXX=MIN0(NC,INT(XX+0.5))
      IYY=MIN0(NR,INT(YY+0.5))
      DX=DD*ABS(COS(PHI))*SIGNX
      DY=DD*ABS(SIN(PHI))*SIGNY
      XX=XX+(DX+RL*DX+RT*DY)/(DELX(IXX))
      YY=YY+(DY+RL*DY-RT*DX)/(DELY(IYY))
      XX=AMIN1(ANC,AMAX1(XX,1.0))
      YY=AMIN1(ANR,AMAX1(YY,1.0))
      IX=MIN0(NC,INT(XX+0.5))
      IY=MIN0(NR,INT(YY+0.5))
      MOVE=MARK(IX,IY)
      IF(MOVE.EQ.0) GO TO 1
```

```
      TABLE(MOVE)=TABLE(MOVE)+PM
      RETURN
2     IX=XX+0.5
      IY=YY+0.5
      NPART(IX,IY)=NPART(IX,IY)+1
      MOVE=0
      RETURN
      END
      SUBROUTINE RDSOLV(EPOR,RHO,KD,RD1)
      REAL KD
      IF(RD1.NE.0) RETURN
      RD1=1+(RHO/EPOR)*KD
      RETURN
      END
      SUBROUTINE SOURCE
      COMMON/EXTRA2/ CH(44,34),HO(44,34),G(44),B(44),R(44,34)
      COMMON/AQUI/ H(44,34),RH(44,34),DELTA,Q(44,34),SOR(44,34)
      COMMON/VEL/ NC,NR,ANC,ANR,V(44,34,2)
      COMMON/POR/ APOR,EPOR,CONSOR(44,34)
      COMMON/POL/ X1,DX,Y1,DY,DELP
      COMMON/TRACE/ NP MAXP,PM
      DO 60 I=1,NC
      DO 50 J=1,NR
      A=0.
      DELSOR=DELP
      RATE=(RH(I,J)-H(I,J))*R(I,J)
      IF(Q(I,J).LT.0.0) RATE=-Q(I,J)
      IF(RATE.LE.0.0) GO TO 50
      IF(CONSOR(I,J).EQ.0.0) GO TO 50
      DELR=SOR(I,J)/RATE
      IF(DELR.GT.DELP) GO TO 40
10    DELSOR=DELSOR-DELR
      XX=I*1.
      YY=J*1.
      DE=DELSOR
      IF(MOVE(XX,YY,DE).EQ.0.0) CALL ADD(XX,YY)
      A=A+1
      IF(A.GT.1) GO TO 20
      P=RATE*(DELP-DELR)*CONSOR(I,J)*8.3453/1E6
20    K=P/PM
      IF(K.LT.1) GO TO 30
      P=P-PM
      DELR=PM*8.3453/(CONSOR(I,J)*8.3453*RATE)
      GO TO 10
30    SOR(I,J)=(PM-P)*1E6/(CONSOR(I,J)*8.3453)
      GO TO 50
40    SOR(I,J)=SOR(I,J)-DELP*RATE
50    CONTINUE
60    CONTINUE
      RETURN
```

```
      END
      SUBROUTINE VELO(XX,YY,VX,VY)
      COMMON/VEL/ NC,NR,ANC,ANR,V(44,34,2)
      LIJ(NR,J,Y)=MIN0(NR-1,MAX0(1,J+IFIX(SIGN(1.0,Y-0.5))))
      I=XX
      IF(I.LE.0) I=1
      IF(I.GE.NC) I=NC-1
      J=YY
      IF(J.LE.0) J=1
      IF(J.GE.NR) J=NR-1
      X=XX-I
      Y=YY-J
      VX=Y*V(I,J+1,2)+(1.-Y)*V(I,J,2)
      VY=X*V(I+1,J,1)+(1.-X)*V(I,J,1)
      JY=LIJ(NR,J,Y)
      IX=LIJ(NC,I,X)
      IF(ABS(VY).LE.1E-30) GO TO 10
      IF(JY.EQ.J) GO TO 10
      YZ=ABS(Y-0.5)
      VY=VY*(1.0-YZ)+YZ*(X*V(I+1,JY,1)+(1.0-X)*V(I,JY,1))
10    IF(IX.EQ.I) GO TO 20
      IF(ABS(VX).LE.1E-20) GO TO 20
      XZ=ABS(X-0.5)
      VX=VX*(1.0-XZ)+XZ*(Y*V(IX,J+1,2)+(1.0-Y)*V(IX,J,2))
20    CONTINUE
      IF(ABS(VX).LE.1E-30) VX=1E-30
      IF(ABS(VY).LE.1E-30) VY=1E-30
      RETURN
      END
```

```
      PROGRAM MK (OUTPUT,TAPE6=OUTPUT)
C*** THIS PROGRAM PRODUCES AN AUTOCORRELATED LOG-NORMAL CONDUCTIVITY
C*** DISTRIBUTION AS DESCRIBED BY FREEZE AND SMITH, (1979).
C
      DIMENSION W(200,200),E(200),Y(200),INTER(200)
      DOUBLE PRECISION DSEED
C*** WKAREA OF DIMENSION GE. NMBLOC**2 + NMBLOC*3
      YMEAN=MEAN OF LOG-NORMAL DISTRIBUTION
      ALPHA=AUTOCORRELATION PARAMETER
      ALPHAZ= AUTOCORRELATION PARAMETER
      NMBLOC=# OF NODES IN F.D. GRID
      NCOL=# OF COLUMNS IN F.D. GRID
      NROW=# OF ROWS IN F.D. GRID
      DSEED=123457.0D0
      YNU=MULTIPLICATION FACTOR USED TO PRODUCE DESIRED STANDARD
     1DEVIATION
      NR=NMBLOC
      L=NMBLOC
      N=NMBLOC
C*** PRODUCE NMBLOC BY NMBLOC MATRIX OF SCALED WEIGHTS
      DO 5 I=1,NMBLOC
      DO 5 J=1,NMBLOC
      W(I,J)=0.0
5     CONTINUE
      W(1,1)=0.0
      W(1,2)=ALPHAX/2.0
      W(1,1+NCOL)=ALPHAZ/2.0
      W(NCOL,NCOL-1)=ALPHAX/2.0
      W(NCOL,NCOL)=0.0
      W(NCOL,NCOL*2)=ALPHAZ/2.0
      W(NMBLOC-(NCOL-1),NMBLOC-(NCOL-1))=0.0
      W(NMBLOC-(NCOL-1),NMBLOC-(2*NCOL-1))=ALPHAZ/2.0
      W(NMBLOC-(NCOL-1),NMBLOC-(NCOL-2))=ALPHAX/2.0
      W(NMBLOC,NMBLOC)=0.0
      W(NMBLOC,NMBLOC-1)=ALPHAX/2.0
      W(NMBLOC,NMBLOC-NCOL)=ALPHAZ/2.0
      IF(NCOL.EQ.2) GO TO 55
      DO 10 I=1,NCOL-1
      W(I,I)=0.0
      W(I,I-1)=ALPHAX/3.0
      W(I,I+1)=ALPHAX/3.0
      W(I,I+NCOL)=ALPHAZ/3.0
10    CONTINUE
      DO 20 I=1,NCOL-2
      W(NMBLOC-(NCOL-1)+I,NMBLOC-(NCOL-1)+I)=0.0
      W(NMBLOC-(NCOL-1)+I,NMBLOC-NCOL+I)=ALPHAX/3.0
      W(NMBLOC-(NCOL-1)+I,NMBLOC-(NCOL-2)+I)=ALPHAX/3.0
      W(NMBLOC-(NCOL-1)+I,NMBLOC-(2*NCOL-1)+I)=ALPHAZ/3.0
20    CONTINUE
      DO 30 I=1,NROW-2
```

```
      W(NCOL+1+NCOL*(I-1),NCOL+1+NCOL*(I-1))=0.0
      W(NCOL+1+NCOL*(I-1),NCOL+2+NCOL*(I-1))=ALPHAX/3.0
      W(NCOL+1+NCOL*(I-1),1+NCOL*(I-1))=ALPHAZ/3.0
      W(NCOL+1+NCOL*(I-1),2*NCOL+1+NCOL*(I-1))=ALPHAZ/3.0
30    CONTINUE
      DO 40 I=1,NROW-2
      W(NCOL+I*NCOL,NCOL+I*NCOL)=0.0
      W(NCOL+I*NCOL,NCOL+I*NCOL-1)=ALPHAX/3.0
      W(NCOL+I*NCOL,I*NCOL)=ALPHAZ/3.0
      W(NCOL+I*NCOL,NCOL+I*NCOL)=ALPHAZ/3.0
40    CONTINUE
      DO 50 I=1,NROW-2
      DO 50 J=1,NCOL-2
      W(I*NCOL+2+(J-1),I*NCOL+2+(J-1))=0.0
      W(I*NCOL+2+(J-1),I*NCOL+2+J)=ALPHAX/4.0
      W(I*NCOL+2+(J-1),I*NCOL+J)=ALPHAX/4.0
      W(I*NCOL+2+(J-1),I*NCOL+1+J-NCOL)=ALPHAZ/4.0
      W(I*NCOL+2+(J-1),I*NCOL+1+J+NCOL)=ALPHAZ/4.0
50    CONTINUE
55    DO 60 I=1,NMBLOC
      W(I,I)=1.0
      DO 60 J=1,NMBLOC
      IF(J.EQ.I) GO TO 60
      W(I,J)=-W(I,J)
60    CONTINUE
C***  INVERT ((I) -(W)) USING GAUSS_JORDAN METHOD, JAMES AND OTHERS (1977).
      DO 212 K=1,NMBLOC
      JJ=K
      IF(K.EQ.NMBLOC) GO TO 206
      KP1=K+1
      BIG=ABS(W(K,K))
      DO 205 I=KP1,NMBLOC
      AB=ABS(W(I,K))
      IF(BIG.GE.AB) GO TO 205
      BOG=AB
      JJ=I
205   CONTINUE
206   INTER(K,1)=K
      INTER(K,2)=JJ
      IF(JJ.EQ.K) GO TO 209
      DO 208 J=1,NMBLOC
      A1=W(K,J)
      A2=W(JJ,J)
      W(K,J)=A2
      W(JJ,J)=A1
208   CONTINUE
209   DO 210 J=1,NMBLOC
      IF(J.EQ.K) GO TO 210
      W(K,J)=W(K,J)/W(K,K)
210   CONTINUE
```

```
      W(K,K)=1./W(K,K)
      DO 211 I=1,NMBLOC
      IF(I.EQ.K) GO TO 211
      DO 211 J=1,NMBLOC
      IF(J.EQ.K) GO TO 211
      W(I,J)=W(I,J) - W(K,J)*W(I,K)
211   CONTINUE
      DO 212 I=1,NMBLOC
      IF(I.EQ.K) GO TO 212
      W(I,K)=-W(I,K)*W(K,K)
212   CONTINUE
      DO 213 L=1,NMBLOC
      K=N-L+1
      KROW=INTER(K,1)
      IROW=INTER(K,2)
      IF(KROW.EQ.IROW) GO TO 213
      DO 213 I=1,NMBLOC
      A1=W(I,KROW)
      A2=W(I,IROW)
      W(I,KROW)=A2
      W(I,IROW)=A1
213   CONTINUE
      CALL GGNML(DSEED,NR,E)
      DO 64 I=1,NMBLOC
64    WRITE(6,65)(W(I,J),J=1,NMBLOC)
65    FORMAT(" ",F6.5,9F7.5)
      DO 70 I=1,NMBLOC
      E(I)=YNU*E(I)
70    CONTINUE
C*** MULTIPLY THE INVERTED MATRIX BY THE RANDOM DISTRIBUTION, N(0,1).
      DO 90 I=1,NMBLOC
      WSUM=0.0
      DO 80 J=1,NMBLOC
      OLDSUM=W(I,J)*E(J)
      WSUM=WSUM+OLDSUM
80    CONTINUE
      Y(I)=WSUM
90    CONTINUE
C*** ADD THE XMEAN TO GET N(YMEAN,YVAR).
      DO 100 I=1,NMBLOC
      Y(I)=Y(I)+YMEAN
100   CONTINUE
      XOLD1=0.0
      XOLD2=0.0
      XOLD3=0.0
      DO 110 I=1,NMBLOC
      VAR1=Y(I)**2
      VAR2=Y(I)
      XMEAN=Y(I)
      XOLD1=XOLD1+VAR1
```

```
      XOLD2=XOLD2+VAR2
      XOLD3=XOLD3+XMEAN
110   CONTINUE
      VAR=(NMBLOC*XOLD1-XOLD2**2)/(NMBLOC*(NMBLOC-1))
      XMEAN=XOLD3/NMBLOC
      WRITE(6,115)
115   FORMAT(///////)
      WRITE(6,117)
117   FORMAT(" ",7X,"VAR",6X,"MEAN")
      WRITE(6,120)VAR,XMEAN
120   FORMAT(" ",2F10.4)
C***  CALCULATE THE INVERSE LOG OF Y(I) TO OBTAIN THE AUTOCORRELATED
C***  LOG-NORMAL CONDUCTIVITY DISTRIBUTION
      DO 130 I=1,NMBLOC
      E(I)=EXP(2.3026*Y(I))
130   CONTINUE
      WRITE(6,135)
135   FORMAT(///)
      WRITE(6,137)
137   FORMAT(" ","HYDRAULIC CONDUCTIVITIES")
      WRITE(6,140)(E(I),I=1,NMBLOC)
140   FORMAT(" ",F6.0,9F7.0)
      STOP
      END
```

```
      PROGRAM MSTAT (INPUT,OUTPUT,TAPE5=INPUT,TAPE6=OUTPUT)
C*** THIS PROGRAM CALCULATES THE MEAN AND STANDARD DEVIATION IN HEAD
C*** AND DISSOLVED CHLORIDE AT EACH NODE IN THE F.D. GRID.  THE # OF
C*** RUNS UPON WHICH THE STATISTICS ARE BASED IS TWENTY
      DIMENSION HEAD(37000),AVE(1500),DEV(1500)
      NRUNS=20
      NDATA=4000
C*** READ 20 VALUES FOR EACH NODE
      READ(5,10)(HEAD(I),I=1,NDATA)
10    FORMAT(10F8.2)
      OLDAV=0.0
      DO 30 I=1,200
      OLDAV=HEAD(I)
      DO 20 J=1,NRUNS-1
      AV=HEAD(I+J*200)+OLDAV
20    OLDAV=AV
      AVE(I)=OLDAV/NRUNS
30    CONTINUE
      OLDEV1=0.0
      OLDEV2=0.0
      DO 50 I=1,200
      OLDEV1=HEAD(I)**2
      OLDEV2=HEAD(I)
      DO 40 J=1,NRUNS-1
      DEV1=HEAD(I+K*200)**2+OLDEV1
      DEV2=HEAD(I+J*200)+OLDEV2
      OLDEV1=DEV1
40    OLDEV2=DEV2
      DEV(I)+SQRT((NRUNS*OLDEV1-OLDEV2**2)/NRUNS**2)
50    CONTINUE
      WRITE(6,60)
60    FORMAT(" ","ARIHMETIC MEAN OF HEAD")
      WRITE(6,70)
70    FORMAT(////)
      WRITE(6,80)(AVE(I),I=1,200)
80    FORMAT(" ",10F8.2)
      WRITE(6,70)
      WRITE(6,90)
90    FORMAT(" ","STANDARD DEVIATION OF HEAD")
      WRITE(6,100)(DEV(I),I=1,200)
100   FORMAT(" ",10F8.2)
      STOP
      END
```

BIBLIOGRAPHY

Bakr, A.A., L.W. Gelhar, A.L. Gutjahr and J.R. MacMillan, 1978, Stochastic analysis of spatial variability in subsurface flows; 1. Comparison of one- and three-dimensional flows: Water Resources Research, 14(2), pp. 263-271.

Bear, J., 1972, Dynamics of Fluids in Porous Media: American Elsevier, New York.

Bear, J., 1979, Hydraulics of Groundwater: McGraw-Hill, New York.

Bennion, D.W. and J.C. Griffiths, 1966, A stochastic model for predicting variations in reservoir rock properties: Trans. AIME, 237, pp. 9-16.

Bridge, J.S. and M.R. Leeder, 1979, A simulation model of alluvial stratigraphy: Sedimentology, 26, pp. 617-644.

Bulnes, A.C., 1946, An application of statistical methods to core analysis data of dolomitic limestone: Trans. AIME, 165, pp. 223-240.

Cooper, H.H., Jr. and C.E. Jacob, 1946, A generalized graphical method for evaluating formation constants and summarizing well field history: Trans. Amer. Geophys. Union, 27, pp. 526-534.

Daniel, W.W., 1977, Introductory Statistics with Applications: Houghton Mifflin Co., Boston.

Davis, S.N., 1969, Flow Through Porous Media: ed. R.J.M. DeWeist, Academic Press, New York, pp. 54-89.

Domenico, P.A. and V.V. Palciauskas, 1979, The volume-averaged mass transport equation for chemical diagenetic model: J. Hydrology, 43, pp. 427-438.

Folk, R.L., 1954, The distinction between grain size and mineral composition in sedimentary-rock nomenclature: J. Geology 62(4), pp. 344-359.

Freeze, R. Allen, 1975, A stochastic conceptual analysis of one-dimensional groundwater flow in nonuniform homogeneous media: Water Resources Research, 11, pp. 725-741.

Freeze, R. Allen and J.A. Cherry, 1979, Groundwater: Prentice-Hall, Inc., Englewood Cliffs, New Jersey.

Freeze, R. Allen and P.A. Witherspoon, 1967, Theoretical analysis of regional groundwater flow: 2. Effect of water table configurations and subsurface permeability variation: Water Resources Research, 3, pp. 623-634.

Galloway, W.E. and W.R. Kaiser, 1980, Catahoula Formation of the Texas Coastal Plain; Origin, geochemical evolution and characteristics of uranium deposits: Texas Bur. Econ. Geol., R.I. 100.

Geogulf, Inc., 1981, Groundwater Quality Assesment, Old Caustic Ponds, Borger, Texas, Report to Phillips Petroleum Company.

Gillham, R.W. and J.A. Cherry, 1982, Contaminant migration in saturated unconsolidated geologic deposits: GSA Special Paper 189, pp. 31-61.

Gustavson, T.C, R.J. Finley and K.A. McGillis, 1980a, Regional dissolution of Permain salt in the Anadarko, Dalhart, and Palo Duro Basins of the Texas Panhandle: Texas Bur. Econ. Geol., R.I. 106.

Gustavson, T.C., M.W. Presley, C.R. Handford, R.J. Finley, S.P. Dutton, R.W. Baumgardner, Jr., K.A. McGillis, and W.W. Simpkins, 1980b, Geology and geohydrology of the Palo Duro Basin, Texas Panhandle; A report on the progress of nuclear waste isolation feasibility studies (1979): Texas Bur. Econ. Geol., Geol. Circ. 80-7.

Hubbert, M.K., 1940, The Theory of Groundwater Motion: J Geology, 48, pp. 785-944.

James, M.L., G.M. Smith, and J.C. Wolford, 1977, Applied Numerical Methods for Digital Computation; With FORTRAN and CSMP: 2nd ed., Harper & Row, New York.

Kessler, L.G., 1971, Characteristics of the braided stream depositional environment with examples from the South Canadian River, Texas: Earth Sci. Bull., 4(1), pp. 25-35.

Law, J., 1944, A statistical approach to the interstitial heterogeneity of sand reservoirs: Trans. AIME, 155, pp. 202-222.

Manford, D., R.M. Dixon, and O.F. Dent, 1974, Reconnaissance investigation of the groundwater resources of the Canadian River Basin, Texas: Texas Board of Water Engineers, Bull. 6016.

McMillan, W.D., 1966, Theoretical analysis of groundwater basin operations: Water Resources Center Contrib., 114.

Mercer, J.W. and C.R. Faust, 1981, Groundwater Modeling: National Water Well Association.

Molz, F.J., O. Guven, and J.G. Melville, 1983, An examination of scale-dependent dispersion coefficients: Ground Water, 21(6), pp. 715-725.

Pickens, J.F. and G.E. Grisak, 1981, Scale-dependent dispersion in a stratified granular aquifer: Water Resources Research, 17(4), pp. 1191-1211.

Pollack, J,M., 1961, Significance of compositional and textural properties of South Canadian River channel sands: New Mexico, Texas, and Oklahoma: J. Sed. Pet., 31(1), pp. 15-37.

Prickett, T.A. and C.G. Lonnquist, 1971, Selected digital computer techniques for groundwater resource evaluation: Illinois State Water Survey, Bull. 55.

Prickett, T.A., T.G. Naymik, and C.G. Lonnquist, 1981, A "random-walk" transport model for selected groundwater quality evaluations: Illinois Dept. Energy and Nat. Sci., Bull. 65.

Reading, H.G., 1978, Sedimentary Environments and Facies: Elsevier, New York.

Richter, B.C., 1983, Geochemical and hydrogeological characteristics of salt spring and shallow subsurface brines in the Rolling Plains of Texas and Southwest Oklahoma: M.A. thesis (unpublished), Univ. Texas at Austin, 147p.

Scheidegger, A.E., 1961, General theory of dispersion in porous media: J. Geophys. Res., 66, pp. 3273-3278.

Schwartz, F.W., 1977, Macroscopic dispersion in porous media; The controlling factors: Water Resources Research, 13(4), pp. 743-752.

Schwartz, F.W. , L. Smith, and A.S. Crowe, 1983, A stochastic analysis of macroscopic dispersion in fractured media: Water Resources Research, 19(5), pp. 1253-1265.

Smith,L. and R.A. Freeze, 1979, Stochastic analysis of steady state groundwater flow in a bounded domain; 2. Two-dimensional simulations: Water Resources Research, 15(6), pp. 1543-1559.

Smith, L. and F.W. Schwartz, 1980, Mass transport; 1. A stochastic analysis of macroscopic dispersion: Water Resources Research, 16(2), pp. 303-313.

Texas Department of Water Resources, Correspondence File SWR 30131, Phillips Petroleum Company;

Trescott, P.C., 1975, Documentation of finite difference model for simulation of three-dimensional groundwater flow: U.S. Geological Survey Open File Report, 75-438.

United States Environmental Protection Services, 1977, The Report to Congress: Waste disposal practices and their effects on groundwater: U.S. Environmental Protection Agency, EPA-570/9-77-002.

Wang, H.F. and M.P. Anderson, 1982, Introduction to Groundwater Modeling: W.A. Freeman and Company, San Fransisco.

Warren, J.E. and H.S. Price, 1961, Flow in heterogeneous porous media: Soc. Petrol. Eng. J., 1, pp. 153-169.

Warren, J.E., F.F. Skiba, and H.S. Price, 1961, An evaluation of the significance of permeability measurements: J. Petrol. Tech., 13, pp. 739-744.

The vita has been removed from the digitized version of this document.